Magnetic dipole excitation as testing field of residual interaction and pairing effect

Tomohiro Oishi

RIKEN Nishina Center, Nuclear Many-body Theory Laboratory

E-mail: tomohiro.oishi@ribf.riken.jp

Contents

Introduction for M1 transitions

Methods = REDF-QRPA

Topics

- M1 with QRPA
- Pairing sensitivity
- Gamow-Teller and M1
- M2 with QRPA

Summary of talk today

Contents

Introduction for M1 transitions

Methods = REDF-QRPA

Topics

- M1 with QRPA
- Pairing sensitivity
- Gamow-Teller and M1
- M2 with QRPA

Summary

M1 transition

Magnetic-dipole (M1) mode is the leading mode of the magnetic excitations by, e.g. electron scattering, proton scattering, etc.

Selection rule: ΔJ=1, Δπ=0, e.g. 0^+(GS) → 1^+.

The M1 response can be a good reference for (i) unnatural-parity residual interactions and (ii) pairing correlations.

Note: the unnatural-parity residual interactions have minor contributions in the even-even ground-state energies, and thus, there remain large ambiguities.

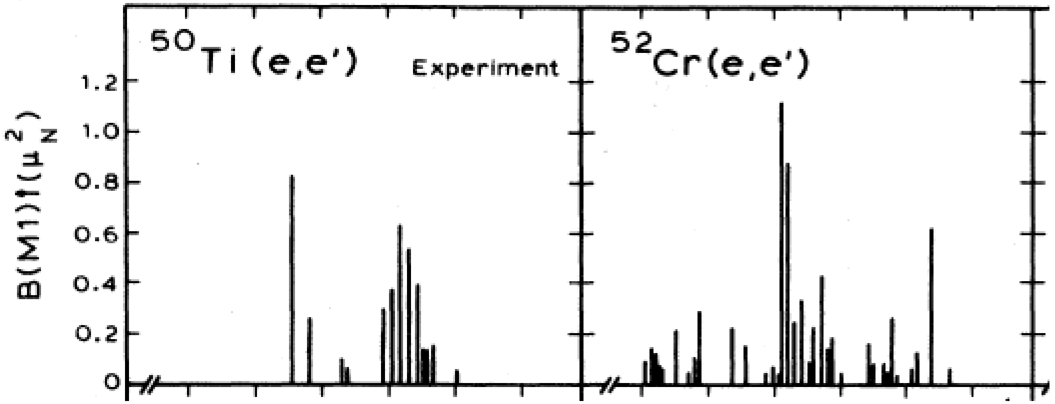

D. I. Sober et al, Phys. Rev. C 31, 2054 (1985).

$$\hat{\mathcal{Q}}(M1,0) = \mu_{\mathrm{N}}\sqrt{\frac{3}{4\pi}}(g_l \hat{l}_0 + g_s \hat{s}_0),$$

$$\hat{\mathcal{Q}}(M1,\pm) = (\mp)\mu_{\mathrm{N}}\sqrt{\frac{3}{4\pi}}(g_l \hat{l}_\pm + g_s \hat{s}_\pm),$$

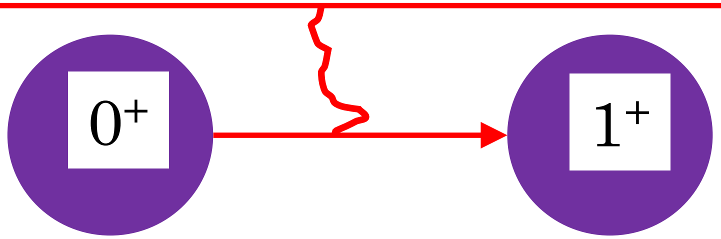

M1 transition: link with neutrino-nuclear reaction

M1 matrix elements can be used to estimate the inelastic neutrino-nuclear scattering, which can be important in astrophysical phenomena, e.g. r-process.
[K. Langanke et. al., PRL 93, 202501 (2004).]

$$\boldsymbol{O}(\mathrm{GT}_0) = \sum_k \boldsymbol{\sigma}(k)\boldsymbol{t}_0(k) = \sum_k 2\boldsymbol{s}(k)\boldsymbol{t}_0(k),$$

$$\boldsymbol{O}(M1)_{\mathrm{iv}} = \sqrt{\frac{3}{4\pi}}\sum_k [\boldsymbol{l}(k)\boldsymbol{t}_0(k) + (g_s^p - g_s^n)\boldsymbol{s}(k)\boldsymbol{t}_0(k)]\mu_N.$$

Inelastic neutrino-nuclear reaction:

$$\sigma_{i,f}(E_\nu) = \frac{G_F^2 g_A^2}{\pi(2J_i+1)}(E_\nu - \omega)^2 |\langle f||\sum_k \boldsymbol{\sigma}(k)\boldsymbol{t}(k)||i\rangle|^2,$$

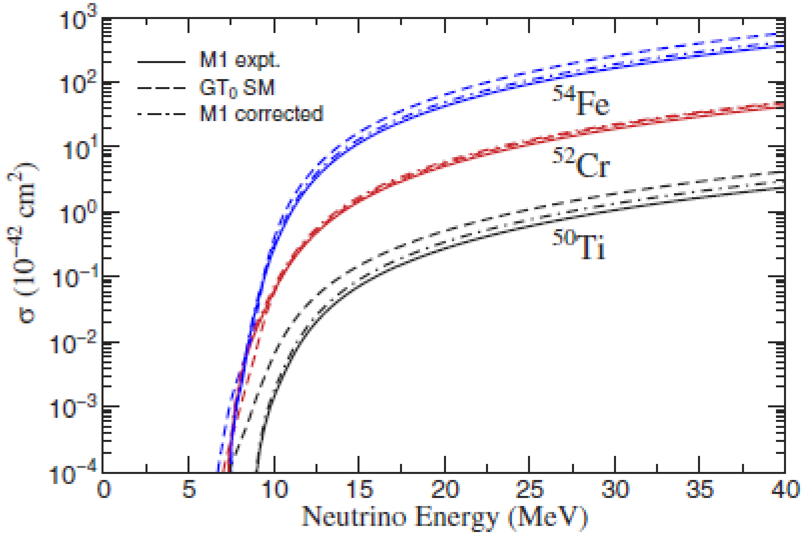

FIG. 2 (color online). Neutrino-nucleus cross sections, calcu-

"Our aim is to show that precision data on the magnetic dipole (M1) strength distributions, obtained by inelastic electron scattering, supply to a large extent the required information about the nuclear Gamow-Teller (GT) distribution which determines the inelastic neutrino-nucleus cross sections for supernova neutrino energies."

M1 transition: link with spin-orbit (LS) splitting

Matrix elements of M1 up to the 1-body-operator level:

$$\hat{\mathcal{Q}}(M1,0) = \mu_{\rm N}\sqrt{\frac{3}{4\pi}}(g_l \hat{l}_0 + g_s \hat{s}_0),$$

$$\hat{\mathcal{Q}}(M1,\pm) = (\mp)\mu_{\rm N}\sqrt{\frac{3}{4\pi}}(g_l \hat{l}_\pm + g_s \hat{s}_\pm),$$

$$\langle \mathcal{Y}_{l'j'} \parallel \hat{s} \parallel \mathcal{Y}_{lj} \rangle = \delta_{l'l}(-)^{l+j'+3/2}\sqrt{(2j'+1)(2j+1)} \begin{Bmatrix} 1/2 & j' & l \\ j & 1/2 & J=1 \end{Bmatrix} \cdot \sqrt{\frac{3}{2}}.$$

$$\left\langle \mathcal{Y}_{l'j'} \parallel \hat{l} \parallel \mathcal{Y}_{lj} \right\rangle = (-)^{l'+j+3/2}\sqrt{(2j'+1)(2j+1)} \begin{Bmatrix} l' & j' & 1/2 \\ j & l & J=1 \end{Bmatrix} \cdot \left\langle Y_{l'} \parallel \hat{l} \parallel Y_l \right\rangle,$$

where $\left\langle Y_{l'} \parallel \hat{l} \parallel Y_l \right\rangle = \delta_{l'l}\sqrt{(2l+1)(l+1)l}.$

M1 operator does not have f(r), and thus, it is expected as sensitive to spin properties.

➔ M1 transition can happen between LS partners, e.g. $f_{7/2}$ → $f_{5/2}$.
Since the nuclear LS splitting is large, M1 becomes measurable.

Proton/electron inelastic scattering to probe M1

A. Tamii et. al., Nucl. Phys. A 788, 53c-60c (2007): M1 excitation by proton inelastic scattering.

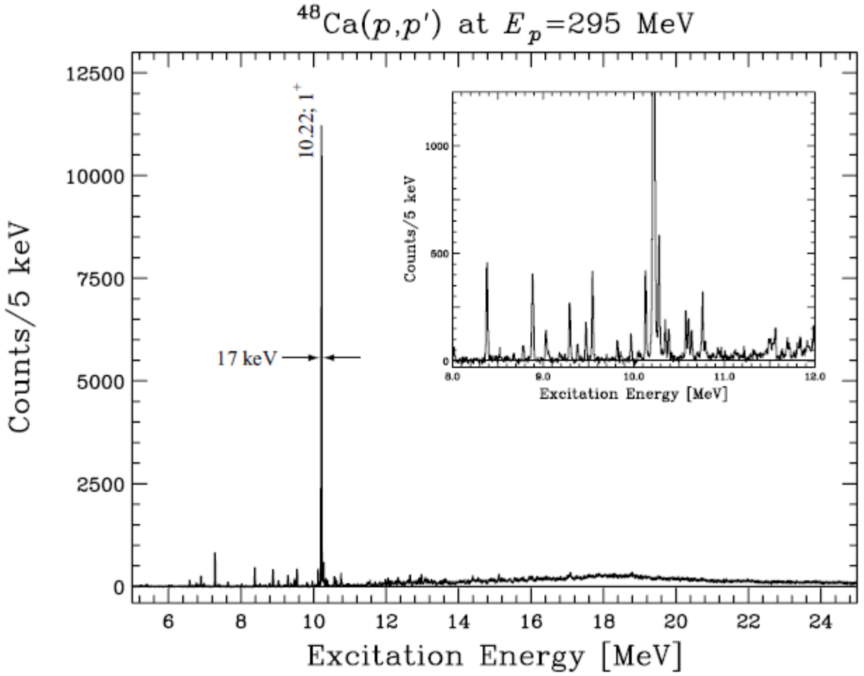

J. Birkhan et. al., PRC 93, 041302(R) (2016).

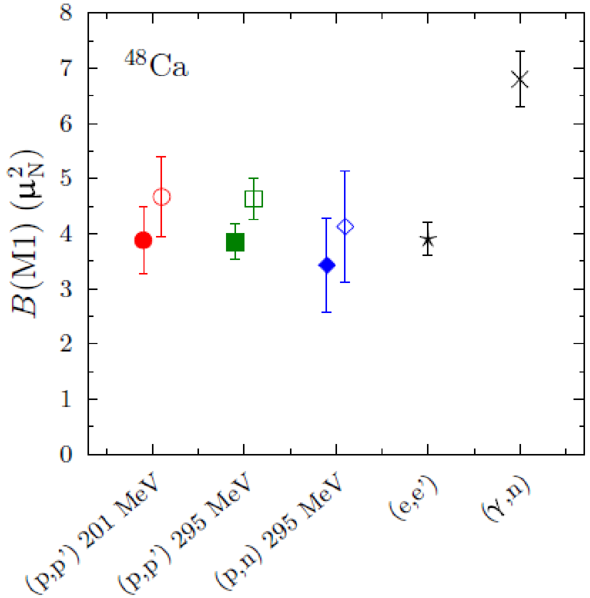

FIG. 4. $B(M1)$ strengths for the transition to the 10.23 MeV state in ^{48}Ca deduced from different experiments. The dependence on the unknown quenching of the IS part in the hadronic reactions is illustrated assuming no quenching (full symbols) or taking the value for IV quenching (open symbols).

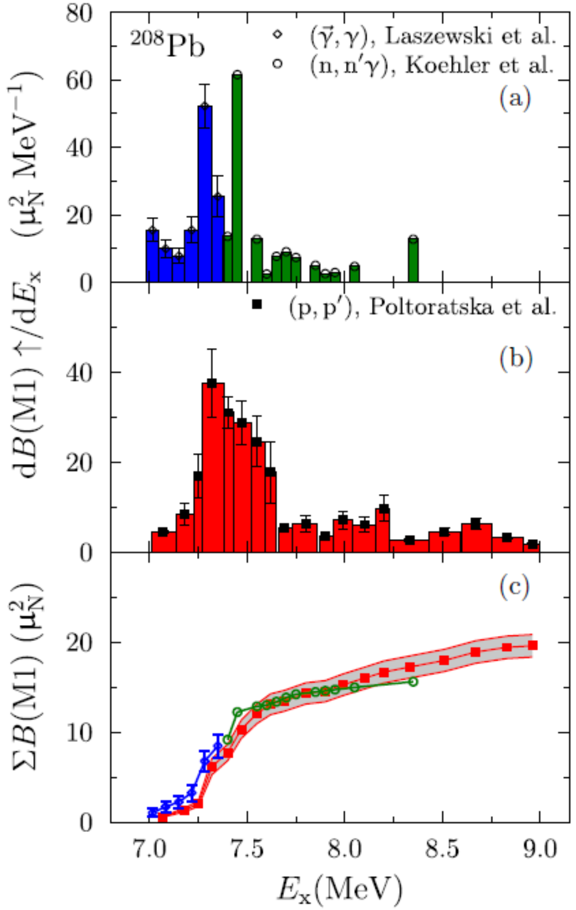

FIG. 3. $B(M1)$ strength distribution in ^{208}Pb between 6.5 and 9 MeV from (a) Refs. [14,15] and (b) the $M1$ proton scattering cross sections of Ref. [34] applying the method described in the present work. (c) Comparison of running sums.

Proton/electron inelastic scattering to probe M1

M. Mathy et. al., PRC 95, 054316 (2017).

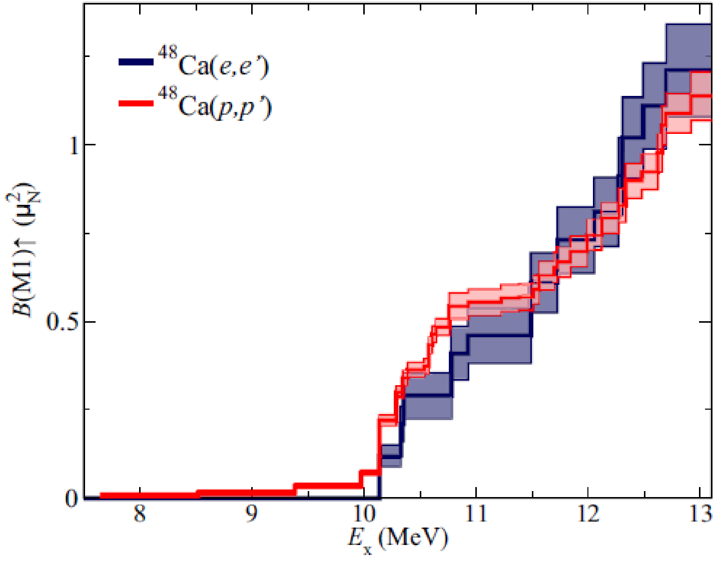

FIG. 9. Running sums of the $B(M1)\uparrow$ strengths in ^{48}Ca between 7 and 13 MeV (excluding the prominent transition to the state at $E_x = 10.23$ MeV) from the (p,p') reaction [present work, red (light grey) histogram] and the (e,e') reaction [Ref. [16], blue (dark gray) histogram]. The bands indicate the experimental uncertainties.

S. Bassauer et. al., Phys. Rev. C 102, 034327 (2020):

M1 data for Sn isotopes are obtained.

TABLE V. Neutron threshold energies S_n, $B(M1)$ strengths up to S_n, and total $B(M1)$ strengths up to energy E_{max} in ^{112,114,116,118,120,124}Sn deduced from the present data as described in the text.

	S_n (MeV)	$\sum_6^{S_n} B(M1)$ (μ_N^2)	E_{max} (MeV)	$\sum_6^{E_{max}} B(M1)$ (μ_N^2)
^{112}Sn	10.79	13.1(1.2)	11.2	14.7(1.4)
^{114}Sn	10.30	9.2(1.0)	12.8	19.6(1.9)
^{116}Sn	9.56	8.1(0.7)	11.8	15.6(1.3)
^{118}Sn	9.32	8.2(1.1)	11.2	18.4(2.4)
^{120}Sn	9.10	4.8(0.5)	12.4	15.4(1.4)
^{124}Sn	8.49	5.6(0.6)	11.4	19.1(1.7)

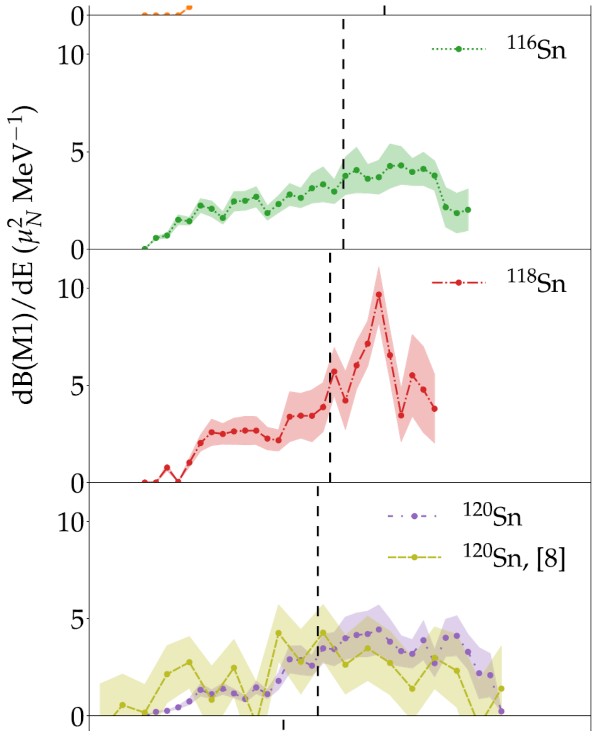

➔ These new data can be a good reference to examine & improve theoretical framework.

Contents

Universal model of nuclei = one dream of nuclear physics

Input		Model		Output
Input = arbitrary set(s) of (Z, N). Z: proton number N: neutron number	→	**Universal Theory for Nuclei**	→	Output = full information on the (Z, N) nucleus, including e.g. 1. Binding energy, 2. Charge and matter radii, 3. Collective excitation, 4. Radioactivity, etc.

Toward this goal, there are several "architypes" in the nuclear theory.
Phenomenological approaches: (continued)

✓ Energy-density functional (EDF) theory for atomic nuclei.
- The practical implementation has been done in the framework of the self-consistent mean-field calculation. The famous example is Hartree-Fock-Bogoliubov (HFB) method.
- Non-relativistic version: Skyrme, Gogny, etc.
- Relativistic version: point-coupling or meson-exchange. ➔ my main topic now.

P.-G. Reinhard, Reports on Progress in Physics 52 (1989) 439.
D. Vretenar, A. V. Afanasjev, G. A. Lalazissis, and P. Ring: Physics Report 409 101 (2005), and references therein.

Universal model of nuclei = one dream of nuclear physics

Input = arbitrary set(s) of (Z, N).
Z: proton number
N: neutron number

→ **Universal Theory for Nuclei** →

Output = full information on the (Z, N) nucleus, including e.g.
1. Binding energy,
2. Charge and matter radii,
3. Collective excitation,
4. Radioactivity, etc.

Toward this goal, there are several “architypes” in the nuclear theory.

- ✓ QCD ➔ The most fundamental theory of strong interaction. However, it is non-perturbative to calculate the low-energy nuclear properties. In future, with e.g. lattice or AdS/CFT, maybe done?

Phenomenological approaches:

- ✓ Shell model: *E. Caurier et. al., Review of Modern Physics 77, 427 (2005);*
  L. Coraggio et. al., Progress in Particle and Nuclear Physics 62(1), 135182 (2009).
- ✓ Ab initio calculation: *S.C. Pieper and R.B. Wiringa, “Quantum Monte Carlo calculations of light nuclei“, Annual Review of Nuclear and Particle Science 51, 5390 (2001);*
  B.R. Barrett, P. Navratil, J.P. Vary, Prog. in Part. and Nucl. Phys. 69, 131181 (2013).
- ✓ Chiral effective field theory:
  R. Machleidt and D.R. Entem, Physics Report 503, 1-75 (2011).

EDF-based meanfield calculation

The nuclear EDF theory has been utilized as one tool to calculate the static and dynamical properties widely in the nuclear chart.

- Non-rela' EDF: Skyrme, Gogny, etc.
- Rela' EDF: meson-exchange, point-coupling, etc.

Implementation:

- Static properties (ground state): the self-consistent EDF-meanfield calc.
- Dynamical properties, e.g. collective excitations: the quasi-particle random-phase approximation (QRPA), time-dependent, etc.

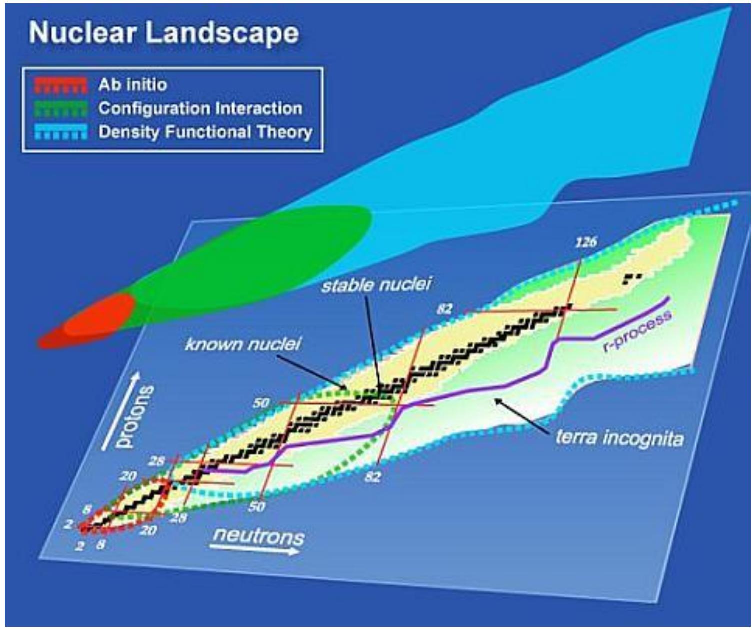

H. Nam et al, J. of Phys. Conf. Series 401, 012033 (2012).

QRPA equation (matrix formulation)

$$\hat{\mathcal{H}}\,|\omega\rangle = E_\omega\,|\omega\rangle\,,$$

$$|\omega\rangle = \hat{\mathcal{Z}}^\dagger(\omega)\,|\Phi\rangle \qquad \hat{\mathcal{Z}}^\dagger(\omega) = \frac{1}{2}\sum_{\rho\neq\sigma}\left\{X_{\rho\sigma}(\omega)\hat{\mathcal{O}}^{(J,P)\dagger}_{\sigma\rho} - Y^*_{\rho\sigma}(\omega)\hat{\mathcal{O}}^{(J,P)}_{\sigma\rho}\right\},$$

$$\begin{pmatrix} A & B \\ B^* & A^* \end{pmatrix}\begin{pmatrix} X(\omega) \\ Y^*(\omega) \end{pmatrix} = \hbar\omega\begin{pmatrix} I & 0 \\ 0 & -I \end{pmatrix}\begin{pmatrix} X(\omega) \\ Y^*(\omega) \end{pmatrix},$$

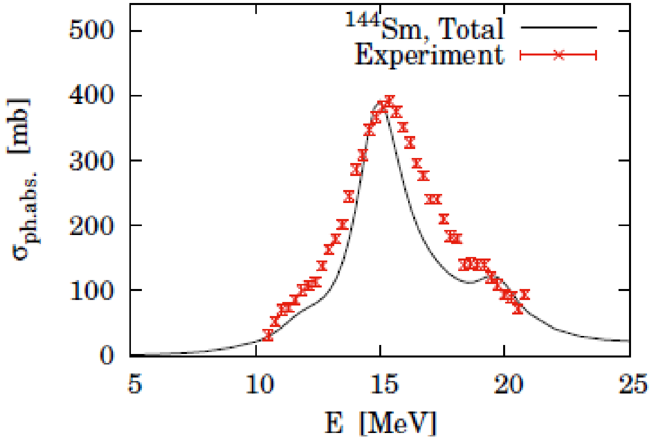

Milestones of nuclear EDF theory

Hohenberg-Kohn theorem (multi-electron systems) Phys. Rev. 136, B844 (1964).
Ground state Φ as well as its energy are functionals of the density $\rho(x) = \langle\Phi|\psi^{+}(x)\psi(x)|\Phi\rangle$. Once the EDF, $\mathrm{E}[\rho(x)] = \langle\Phi[\rho]|\hat{H}|\Phi[\rho]\rangle$ is found, the ground state can be solved by the density-variational principle.

Kohn-Sham method (multi-electron systems) Phys. Rev. 140, A1133 (1965).
Implementation of the density-variational principle is shown as applicable.

EDF theory for multi-nucleon systems

- (1970~) Phenomenological self-consistent meanfield calculations with Skyrme, Gogny, Rela' point-coupling, etc. E.g. D. Vautherin and D. M. Brink, Phys. Rev. C 5, 626 (1972).
- (2000~) Those meanfield calculations are re-considered as the products of nuclear EDF theory.

Methods:

(i) REDF-based Hartree-Bogoliubov
(ii) quasi-particle random-phase approximation (QRPA)

Point-Coupling REDF Lagrangian

In the relativistic nuclear theory (RNT), nucleon is described by a Dirac spinor $\psi(x)$, where $x = \{\boldsymbol{r}, \boldsymbol{s}, \vec{\tau}\}$. The phenomenological Lagrangian density reads

$$\mathcal{L} = \bar{\psi}(x)[i\gamma_\mu \partial^\mu - M]\psi(x) + \mathcal{L}_{\rm M} + \mathcal{L}_{\rm I}. \qquad (1)$$

TABLE 2: Interaction terms included in $\mathcal{L}_{\rm I}$. Label (i) indicates isoscalar (IS) or isovector (IV). Label (ii) indicates scalar (S), vector (V), pseudo-scalar (PS) or pseudo-vector (PV).

(i)	(ii)	(T, J^π)	Meson	Meson-exchange	Point-coupling
IS	S	$(0, 0^+)$	σ	$-g_\sigma \bar{\psi}\sigma\psi$	$-\alpha_{\rm IS-S}(\rho)[\bar{\psi}\psi][\bar{\psi}\psi]/2$
					$-\delta_{\rm IS-S}(\rho)\partial_\mu[\bar{\psi}\psi]\partial^\mu[\bar{\psi}\psi]/2$
	V	$(0, 1^-)$	ω^μ	$-g_\omega[\bar{\psi}\gamma_\mu\omega^\mu\psi]$	$-\alpha_{\rm IS-V}(\rho)[\bar{\psi}\gamma_\mu\psi][\bar{\psi}\gamma^\mu\psi]/2$
	PS	$(0, 0^-)$	$\times$	$\times$	$\times$
	PV	$(0, 1^+)$	$\times$	$\times$	$\times$
IV	S	$(1, 0^+)$	$\times$	$\times$	$\times$
	V	$(1, 1^-)$	$\vec{\rho}^\mu$	$-g_\rho[\bar{\psi}\gamma_\mu(\vec{\tau}\vec{\rho}^\mu)\psi]$	$-\alpha_{\rm IV-V}(\rho)[\bar{\psi}\gamma_\mu\vec{\tau}\psi][\bar{\psi}\gamma^\mu\vec{\tau}\psi]/2$
	PS	$(1, 0^-)$	$\vec{\pi}$	$-ig_\pi[\bar{\psi}\gamma_5(\vec{\tau}\vec{\pi})\psi]$	$-\alpha_{\rm IV-PS}(\rho)[\bar{\psi}\gamma_5\vec{\tau}\psi][\bar{\psi}\gamma_5\vec{\tau}\psi]/2$
	PV	$(1, 1^+)$	$\partial_\mu\vec{\pi}$	$-\frac{f_\pi}{m_\pi}[\bar{\psi}\gamma_5\gamma_\mu\partial^\mu(\vec{\tau}\vec{\pi})\psi]$	$-\alpha_{\rm IV-PV}(\rho)[\bar{\psi}\gamma_5\gamma_\mu\vec{\tau}\psi][\bar{\psi}\gamma_5\gamma^\mu\vec{\tau}\psi]/2$
Coulomb					$-e\bar{\psi}\gamma_\mu A^\mu\left(\frac{1-\hat{\tau}_3}{2}\right)\psi$

In this work, we employ the point-coupling model.

Setting = DD-PC1 parameters.

References:

[1] T. Niksic, D. Vretenar, and P. Ring, Progress in Particle and Nuclear Physics 66(3), 519-548 (2011). [2] T. Niksic et. al., Comp. Phys. Communications, 107184 (2020).

Relativistic Hartree method

※Fock term is neglected, and DD-PC1 parameters are re-optimized.

For example, DD-PC1 Lagrangian ➔ DD-PC1 Hamiltonian. $\mathcal{H}(x) \equiv \left(\partial_0 \psi^\dagger\right) \frac{\delta \mathcal{L}}{\delta\left(\partial_0 \psi^\dagger\right)} + \frac{\delta \mathcal{L}}{\delta\left(\partial_0 \psi\right)} \left(\partial_0 \psi\right) - \mathcal{L}$

(1) We assume the relativistic Hartree ground-state solution as single-Slater determinant of the particle-basis states.

$$|\mathrm{HF}\rangle = c_A^\dagger \cdots c_1^\dagger \, |-\rangle.$$

Then, the Hamiltonian is also formally represented within these basis:

$$H(t) = \sum_{r,s} \int dE' \int dE \int d^3\boldsymbol{r}$$
$$\left[u^\dagger_{r,E'}(x) c^\dagger_{r,E'} + v^\dagger_{r,-E'}(x) b^\dagger_{r,-E'}\right] \hat{h}_D \left[u_{s,E}(x) c_{s,E} + v_{s,-E}(x) b_{s,-E}\right]$$

(2) No-sea approximation: we neglect the Dirac-sea states with negative energies.

(3) The particle states are obtained from the self-consistent mean-field Dirac equation:

Initial guess: $\psi_N(\boldsymbol{r})$ → Densities → Potentials (scalar & vector) → Dirac equation (from variation principle):

$$\left[-i\hbar c \beta \vec{\gamma} \cdot \vec{\nabla} + \beta M c^2 + \beta S(r) + W(r)\right] \psi_N(t, \boldsymbol{r}) = E_N \psi_N(t, \boldsymbol{r}).$$

→ $\psi_{nljm}(\boldsymbol{r}) = \begin{pmatrix} iF_N(\boldsymbol{r}) \\ G_N(\boldsymbol{r}) \end{pmatrix}$ → Densities

Bogoliubov transformation for pairing

$c_k^\dagger$ & $c_k \cdots$ Original creation & annihilation,
$a_k^\dagger$ & $a_k \cdots$ QP creation & annihilation.

Hamiltonian in the true-particle representation: $$\hat{\mathcal{H}} = \sum_{kl} \epsilon_{kl} c_k^\dagger c_l + \frac{1}{4} \sum_{a \neq b} \sum_{c \neq d} \tilde{v}_{ab,cd} \left(c_b c_a\right)^\dagger c_d c_c,$$

(1) Before the Bogoliubov transformation = pairing correlation, the HF-ground state is obtained as single-Slater determinant of the true-particle states. $$|\mathrm{HF}\rangle = c_A^\dagger \cdots c_1^\dagger |-\rangle.$$

(2) Then we move to the HFB-ground state by the Bogoliubov transformation.

$$\begin{pmatrix} a_\downarrow \\ a_\downarrow^\dagger \end{pmatrix} = \begin{pmatrix} U^\dagger & V^\dagger \\ V^T & U^T \end{pmatrix} \begin{pmatrix} c_\downarrow \\ c_\downarrow^\dagger \end{pmatrix} \equiv \hat{\mathcal{W}}^\dagger \begin{pmatrix} c_\downarrow \\ c_\downarrow^\dagger \end{pmatrix}$$

These Bogoluibov coefficients (U & V) are determined so as to minimize the <H> including the pairing gap.
How to solve them numerically? ➔ H(F)B equation.

$$\sum_l \begin{pmatrix} h & \Delta \\ -\Delta^* & -h^* \end{pmatrix}_{kl} \begin{pmatrix} U_{lm} \\ V_{lm} \end{pmatrix} = \delta_{km} E_m \begin{pmatrix} U_{km} \\ V_{km} \end{pmatrix}.$$

$$h_{kl} = \epsilon_{kl} + \Gamma_{kl}, \quad \Gamma_{kl} = \sum_{pq} \tilde{v}_{kq,lp} \rho_{pq},$$

$$\Delta_{kl} = \frac{1}{2} \sum_{pq} \tilde{v}_{kl,pq} \kappa_{pq}.$$

$$\rho_{kl} \equiv \left\langle \Phi \mid c_l^\dagger c_k \mid \Phi \right\rangle,$$

$$\kappa_{kl} \equiv \langle \Phi \mid c_l c_k \mid \Phi \rangle,$$

Quasi-particle random-phase approximation (QRPA)

[0] Hartree-(Fock)-Bogoliubov solves the ground state of quasi-particles. Then the excited states are generally given as follows.

$$\hat{\mathcal{H}} \left|\omega\right\rangle = E_\omega \left|\omega\right\rangle, \quad \left|\omega\right\rangle = \hat{\mathcal{Z}}^\dagger(\omega) \left|\Phi\right\rangle \quad \Longleftrightarrow \quad \left[\hat{\mathcal{H}},\ \hat{\mathcal{Z}}^\dagger(\omega)\right] = \hbar\omega \hat{\mathcal{Z}}^\dagger(\omega), \quad \left[\hat{\mathcal{H}},\ \hat{\mathcal{Z}}(\omega)\right] = -\hbar\omega \hat{\mathcal{Z}}(\omega),$$

$$\hat{\mathcal{W}}(t) \equiv \hat{\mathcal{Z}}^\dagger(\omega) e^{-i\omega t} - \hat{\mathcal{Z}}(\omega) e^{i\omega t}, \quad i\hbar \frac{\partial}{\partial t} \hat{\mathcal{W}}(t) = \left[\hat{\mathcal{H}},\ \hat{\mathcal{W}}(t)\right]$$

[1] QRPA assumption: we only consider the one-body-operator type, where its spin-parity couples to (J, P).

$$\hat{\mathcal{Z}}^\dagger(\omega) = \frac{1}{2} \sum_{\rho \neq \sigma} \left\{ X_{\rho\sigma}(\omega) \hat{\mathcal{O}}_{\sigma\rho}^{(J,P)\dagger} - Y^*_{\rho\sigma}(\omega) \hat{\mathcal{O}}_{\sigma\rho}^{(J,P)} \right\}, \quad \text{where } \hat{\mathcal{O}}_{\sigma\rho}^{(J,P)} = [a_\sigma \otimes a_\rho]^{(J,P)}$$

[2] Amplitudes (X & Y) can be obtained from the matrix QRPA equation.

$$\begin{pmatrix} A & B \\ B^* & A^* \end{pmatrix} \begin{pmatrix} X(\omega) \\ Y^*(\omega) \end{pmatrix} = \hbar\omega \begin{pmatrix} I & 0 \\ 0 & -I \end{pmatrix} \begin{pmatrix} X(\omega) \\ Y^*(\omega) \end{pmatrix},$$

$$A_{ab,cd} \equiv \left\langle \Phi \left[a_b a_a,\ \mathcal{H} a_c^\dagger a_d^\dagger - a_c^\dagger a_d^\dagger \mathcal{H} \right] \Phi \right\rangle, \\ = (E_a + E_b)\delta_{ac}\delta_{bd} + H^{22}_{ab,cd},$$

$$B_{ab,cd} \equiv (-) \left\langle \Phi \left[a_b a_a,\ \mathcal{H} a_d a_c - a_d a_c \mathcal{H} \right] \Phi \right\rangle \\ = 4! \cdot H^{40}_{abcd},$$

➔ QRPA matrices A & B are determined from the effective interaction (Lagrangian). Those are numerically calculated and diagonalized.

➔ Note that the numerical cost can be a problem.

What "relativistic" EDF provides?

Relativistic EDF (Covariant DF) Theory
= effective field theory of nucleons and mesons.

$$
\begin{aligned}
\mathcal{L}_{\rm REDF} &= \bar{\psi}(x)\left[i\,\partial\!\!\!/ - m\right]\psi(x) \\
&\quad + \mathcal{L}_{\rm meson} + \mathcal{L}_{\rm int}, \quad \text{where} \\
\psi(x) &\cdots \text{nucleon}, \\
\mathcal{L}_{\rm meson} &\cdots \text{free mesons}, \\
\mathcal{L}_{\rm int} &\cdots \text{interactions}.
\end{aligned}
$$

Motivation & Caution to choose the REDF framework:

- ✓ In the original work by J.D. Walecka [1], his original motivation was to obtain the stress tensor for the Einstein equation of neutron stars. This purpose needs the relativistic formalism. As a successful result by Walecka [1], the repulsive core of the nuclear force in the high-density region can be naturally concluded.
- ✓ The Dirac-Lorentz formalism leads to a consistent treatment of spin degrees of freedom as well as an unified description of time-even and time-odd fields [2]. Also, the relativistic effect and causality can be included [1-4].
- ✓ Connection between the force and meson is clear: e.g. tensor force is from one-pion exchange (pseudo-scalar & pseudo-vector coupling) [4].
- ✓ Spin-orbit (LS) level splitting, which is one fundamental feature of atomic nuclei, is naturally concluded [2-4]. This character could be a key to evaluate e.g. the charge distribution, M1 and Gamow-Teller excitations, etc.

References: [1] J. D. Walecka, Ann. of Phys. 83, 491 (1974); [2] D. Vretenar et al., Phys. Report 409, 101-259 (2005); [3] P.-G. Reinhard, Rep. on Progress in Phys. 52, 439 (1989); [4] 土岐博＆保坂淳、「相対論的多体系としての原子核」、大阪大学出版会(2011).

Spin-orbit (LS) splitting from Dirac eq.

$$\left[-i\hbar c\beta\vec{\gamma}\cdot\vec{\nabla}+\beta Mc^2+\beta S(r)+W(r)\right]\psi_N(t,\boldsymbol{r})=E_N\psi_N(t,\boldsymbol{r}).$$

Scalar meson(s)

Vector meson(s)

$$\psi_N(\boldsymbol{r})=\psi_{nljm}(\boldsymbol{r})=\begin{pmatrix} iF_N(\boldsymbol{r}) \\ G_N(\boldsymbol{r}) \end{pmatrix}=\begin{pmatrix} if_{nlj}(r)\mathcal{Y}_{ljm}(\bar{\boldsymbol{r}}) \\ g_{nlj}(r)\frac{\vec{\sigma}\cdot\boldsymbol{r}}{r}\mathcal{Y}_{ljm}(\bar{\boldsymbol{r}}) \end{pmatrix}$$

$$\left[-\frac{(\hbar c)^2}{\epsilon_N(r)}\nabla^2-(\hbar c)^2\frac{(-)\epsilon'_N(r)}{\epsilon_N^2(r)}\frac{d}{dr}+\frac{(\hbar c)^2}{r}\frac{(-)\epsilon'_N(r)}{\epsilon_N^2(r)}\frac{2\vec{S}\cdot\vec{L}}{\hbar^2}\right.$$
$$\left.+S(r)+W(r)\right]F_N(\boldsymbol{r}) = (E_N-Mc^2)F_N(\boldsymbol{r}),$$

where the 1st term in the LHS corresponds to the kinetic energy, the 2nd term is so-called Darwin term, and the 3rd term indicates the spin-orbit coupling. These Darwin and spin-orbit terms can be naturally concluded from the Dirac equation, whereas those were just introduced as "phenomenology" in the Schroedinger equation.

It is convenient to find that,

- the total potential is given as $S(r)+W(r)$, whereas,
- the spin-orbit and Darwin terms depend on the $\epsilon'_N(r)=S'(r)-W'(r)$.

Contents

Relativistic QRPA for M1

Publications:

1. G. Kruzic, T.O., D. Vale, and N. Paar, Phys. Rev, C 102, 044315 (2020);
2. T.O., G. Kruzic, and N. Paar, J. Phys. G 47, 115106 (2020);
3. G. Kruzic, T.O., and N. Paar, PRC 103, 054306 (2021).

Rela’ Hartree-Bogoliubov & QRPA

Point-coupling REDF Lagrangian: $\mathcal{L} = \bar{\psi}(x)[i\gamma_\mu \partial^\mu - M]\psi(x) + \mathcal{L}_{\rm M} + \mathcal{L}_{\rm I}.$

$$\mathcal{L}_I = \boxed{-\frac{\alpha_{\rm IS-S}(\rho)}{2}[\bar{\psi}\psi][\bar{\psi}\psi] - \frac{\alpha_{\rm IS-V}(\rho)}{2}[\bar{\psi}\gamma_\mu\psi][\bar{\psi}\gamma^\mu\psi] - \frac{\alpha_{\rm IV-V}(\rho)}{2}[\bar{\psi}\gamma_\mu\vec{\tau}\psi][\bar{\psi}\gamma^\mu\vec{\tau}\psi]} \text{ DD-PC}$$

$$\boxed{-\frac{\alpha_{\rm IV-PV}(\rho)}{2}[\bar{\psi}\gamma_5\gamma_\mu\vec{\tau}\psi][\bar{\psi}\gamma_5\gamma^\mu\vec{\tau}\psi]} - e\bar{\psi}\gamma_\mu A^\mu\left(\frac{1-\hat{\tau}_3}{2}\right)\psi$$

IV-PV for QRPA

- ✓ (i) For the GS of even-even nuclei, the relativistic Hartree-Bogoliubov (RHB) calculation is performed by using the DD-PC setting for Lagrangian [1, 2]. (ii) Two-Gaussian pairing force is employed in the particle-particle channel [3]. (iii) For the M1-excited states, the QRPA is employed [3].

QRPA: $\frac{dB_{\rm M1}}{dE_\gamma} = \sum_i \delta(E_\gamma - \hbar\omega_i)\sum_\nu \left|\left\langle \omega_i \middle| \hat{Q}_\nu({\rm M1}) \middle| \Phi\right\rangle\right|^2$ from $\begin{pmatrix} A & B \\ B^* & A^* \end{pmatrix}\begin{pmatrix} X(\omega) \\ Y^*(\omega) \end{pmatrix} = \hbar\omega \begin{pmatrix} I & 0 \\ 0 & -I \end{pmatrix}\begin{pmatrix} X(\omega) \\ Y^*(\omega) \end{pmatrix},$

- ✓ (iv) In the QRPA, we additionally consider the IV-PV coupling as the residual interaction [3]. Note that this IV-PV originates in the one-pion exchange.

References: [1] T. Niksic, D. Vretenar, and P. Ring, Progress in Particle and Nuclear Physics 66(3), 519-548 (2011). [2] T. Niksic et. al., Comp. Phys. Com., 107184 (2020). [3] G. Kruzic et. al., PRC 102, 044315 (2020).

How about the ground-state (GS) properties?

Relativistic EDF (Covariant DF) Lagrangian
= density-dependent point-coupling (DD-PC) effective field theory of nucleons.

$$\mathcal{L} = \mathcal{L}_{\mathrm{DD-PC1}} + \mathcal{L}_{\mathrm{IV-PV}},$$

\+

- Self-consistent mean-field assumption for single Slater determinant of (quasi-particle) A nucleons.
- For the pp channel, the driving force of Cooper-pairing correlation is approximated with the non-relativistic finite-range force.
- We neglect the Fock terms, and re-optimize the DD-PC Lagrangian. ➔ Self-consistent Dirac-Hartree-Bogoliubov calculation with HO basis.

✓ One relativistic-synonym method of calculation, which is similar to the HFB with Skyrme or Gogny force.

✓ Binding energies, their odd-even staggering, and charge radii of medum-heavy nuclei can be well reproduced.

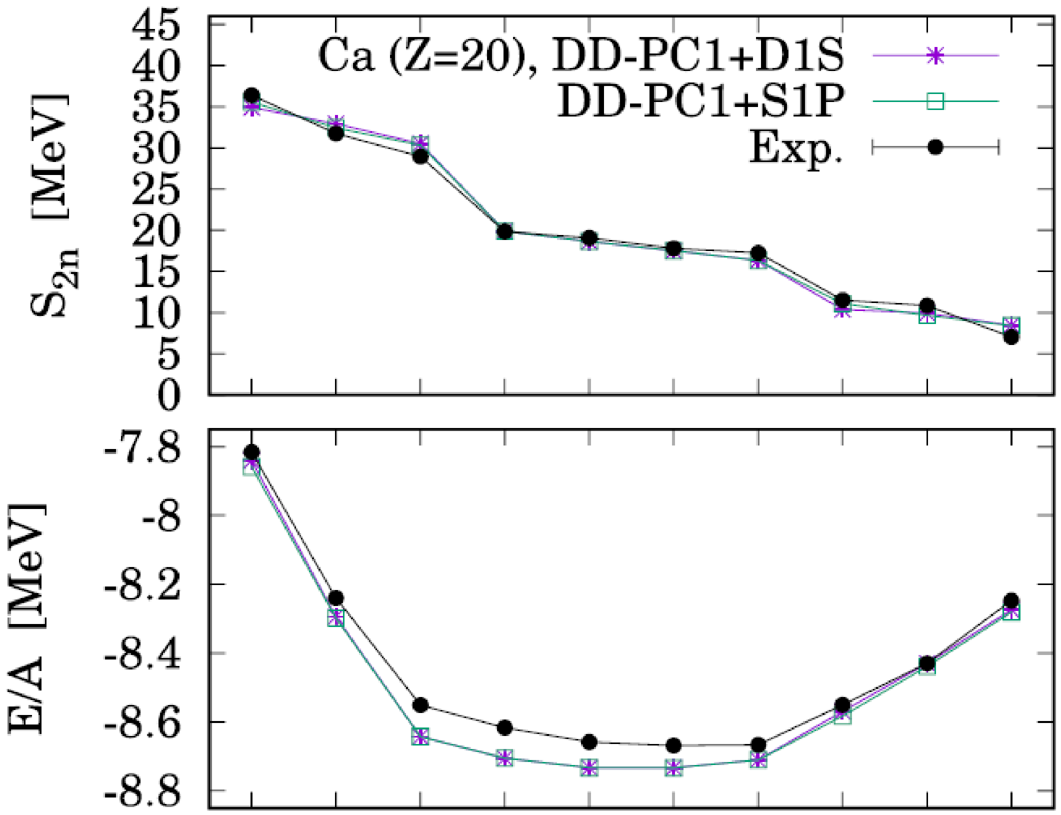

Residual interactions to shift M1 energies

$$\frac{dB_{M1}}{dE_\gamma} = \sum_f \delta(E_\gamma - \hbar\omega_f) \sum_\nu \left| \left\langle \omega_f | \hat{Q}_\nu(\mathrm{M1}) | \Phi \right\rangle \right|^2,$$

$$\hat{Q}_\nu^{(\mathrm{IV})} = \sqrt{\frac{3}{4\pi}} \mu_\mathrm{N} \sum_{i \in A} \left[g_l^{(\mathrm{IV})} \hat{l}_\nu(i) + g_s^{(\mathrm{IV})} \hat{s}_\nu(i) \right] \hat{\tau}_3(i),$$

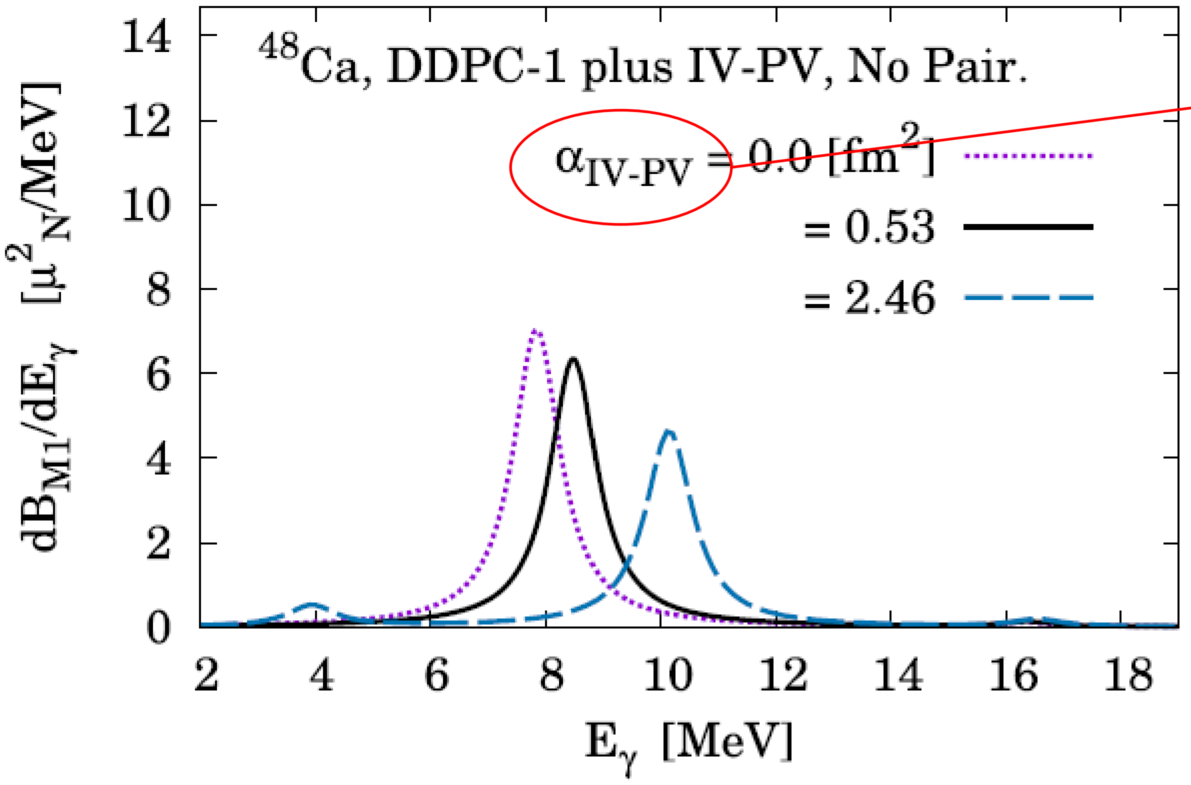

$$\mathcal{L}_{\mathrm{IV-PV}} = -\hbar c \frac{\alpha_{\mathrm{IV-PV}}}{2} \left[\bar{\psi} \gamma_5 \gamma_\mu \vec{\tau} \psi \right] \left[\bar{\psi} \gamma_5 \gamma^\mu \vec{\tau} \psi \right]$$

Interactions:
(1) DD-PC1 for ph-RHB;
(2) IV-PV (residual int.) for ph-RQRPA.

➔ The IV-PV unnatural-parity residual interaction significantly affects the M1 response. Note that, if we only see the GS (0+) solution from the RHB, the IV-PV does not make a finite effect.

Residual interactions to shift M1 energies

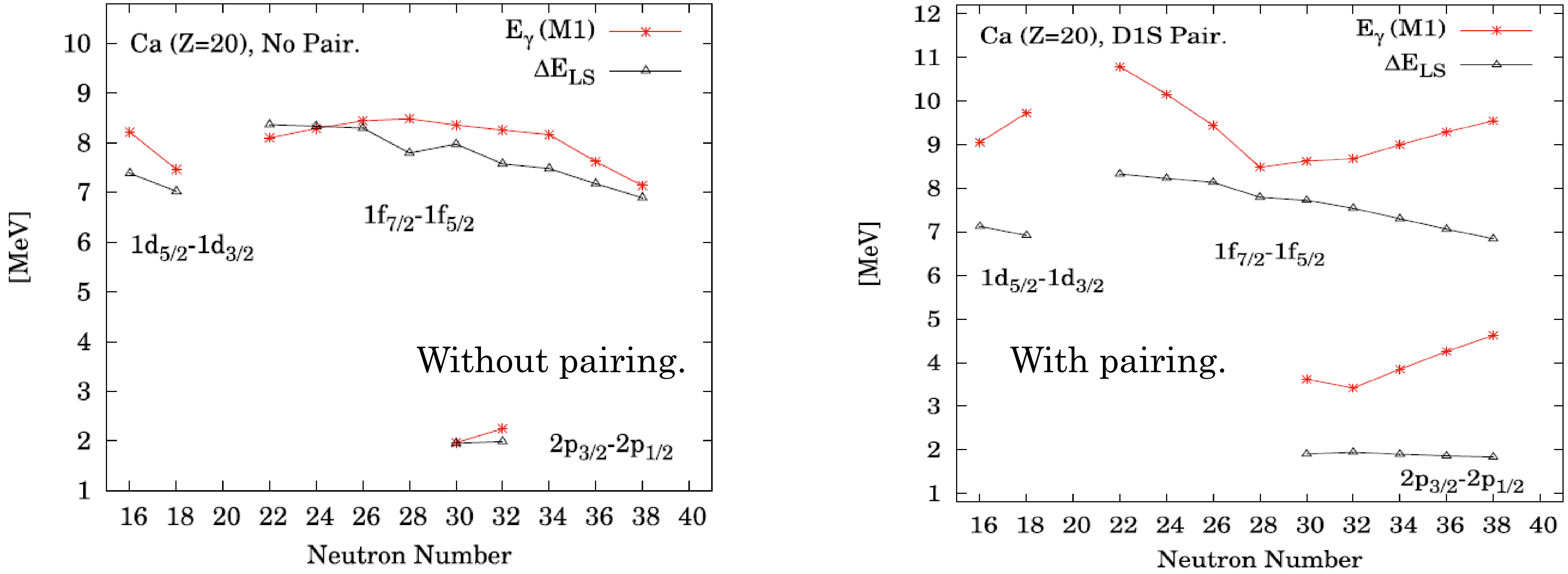

- ✓ The IV-PV interaction causes the actual M1-excitation energy to shift from the original LS-splitting energy for a few MeV.
- ✓ In addition, the pairing interaction (right panel) also provides the finite shift of the M1 energy from the LS-splitting.

Summation of IV M1 strength

Sumrule: $m_k(\mathrm{M1}) \equiv \int E_\gamma^k \frac{dB_{\mathrm{M1}}}{dE_\gamma}\, dE_\gamma.$

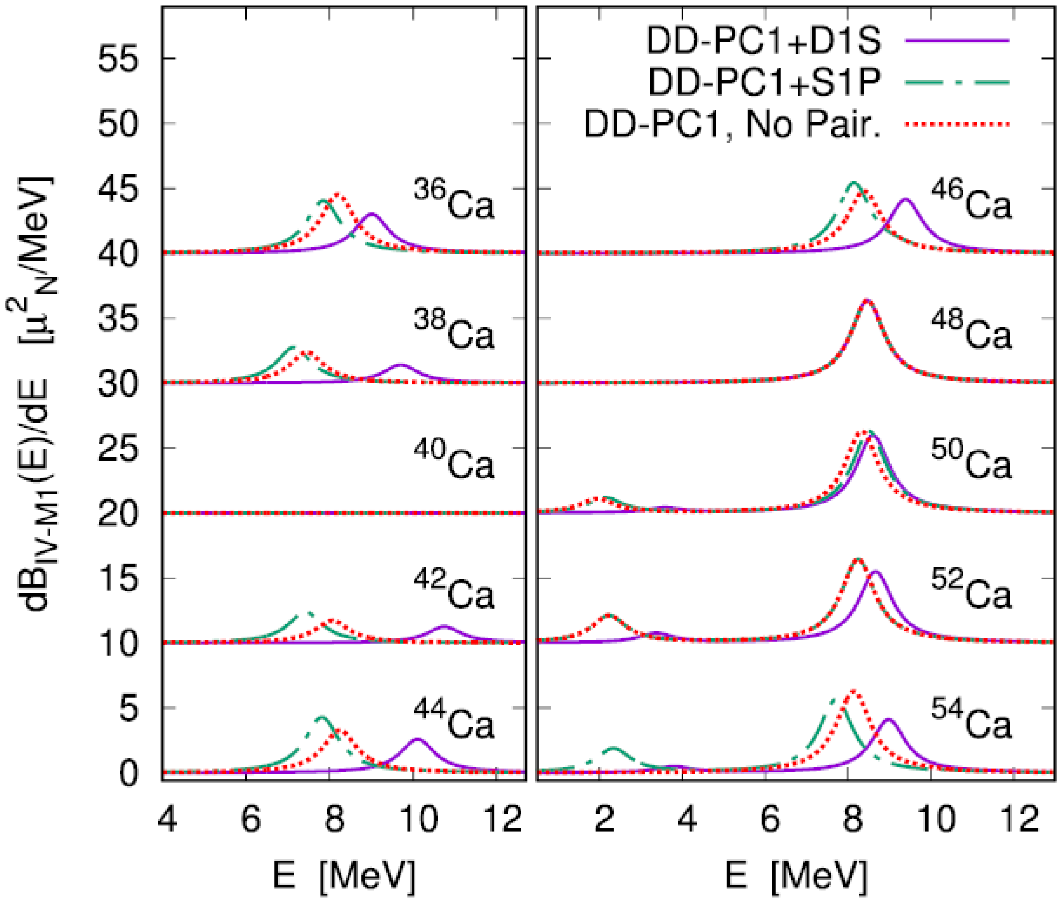

Fig. 3 The IV-M1 strength ($0^+_{\mathrm{GS}} \longrightarrow 1^+$) in the DD-PC1 plus D1S pairing, plus S1P pairing, and no pairing cases for Ca isotopes

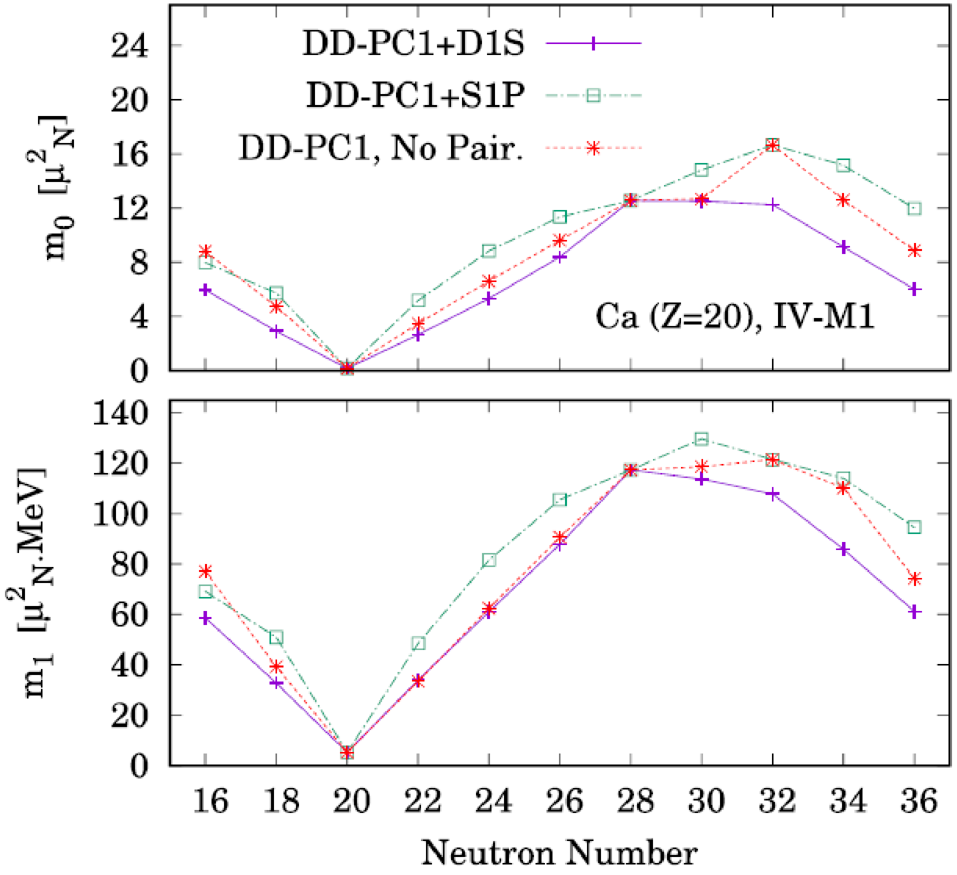

Fig. 4 (Top) Non-energy-weighted summation m_0 of the M1 strength in the DD-PC1 plus D1S pairing, +S1P pairing, and no pairing cases. (Bottom) Same but for the energy-weighted summation m_1

➔ For open-shell nuclei, the pairing interaction affects the M1 strength.

Quenching effect in M1

G. Kruzic, T.O., N. Paar, PRC 103, 054306.

We performed the systematic evaluation of M1 in Sn isotopes:

Our REDF-QRPA result

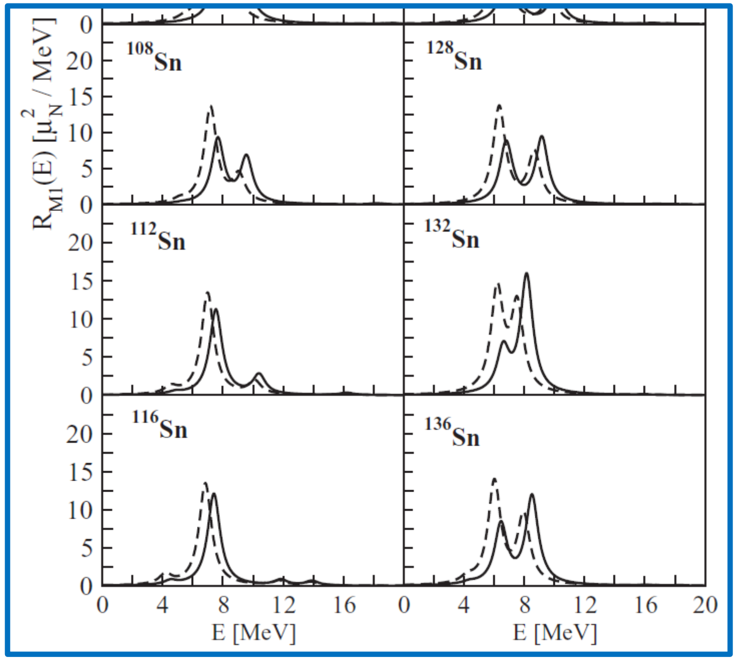

➔ Summation of M1 strength:

	$\sum B_{M1}^{th.}$	$\sum B_{M1}^{exp.}$	g_{eff}/g_{free}
^{112}Sn	22.81	14.7(1.4)	0.80
^{114}Sn	22.61	19.6(1.9)	0.93
^{116}Sn	22.56	15.6(1.3)	0.83
^{118}Sn	22.76	18.4(2.4)	0.89
^{120}Sn	23.34	15.4(1.4)	0.81
^{124}Sn	25.55	19.1(1.7)	0.86

Exp. Data from S. Basseur et. al., PRC 102, 034327 (2020).

✓ Quenching of 0.8-0.9 is necessary to reproduce the exp. M1 summation, i.e., it is not bad.

✓ Note that the experimental M1 distribution is quite broad, whereas our result is based on a narrow-resonance assumption.

Contents

Magnetic-dipole (M1) excitation of nuclear Cooper pair

$$\boxed{\hat{\mathcal{O}}_{M1} = g_s[\hat{s}_1 + \hat{s}_2] + g_l[\hat{l}_1 + \hat{l}_2]}$$

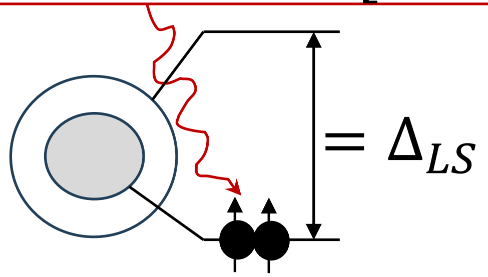

$B_{M1}(E_\gamma; 0+ \longrightarrow 1+)$, $E_\gamma = E_f - E_{GS}$

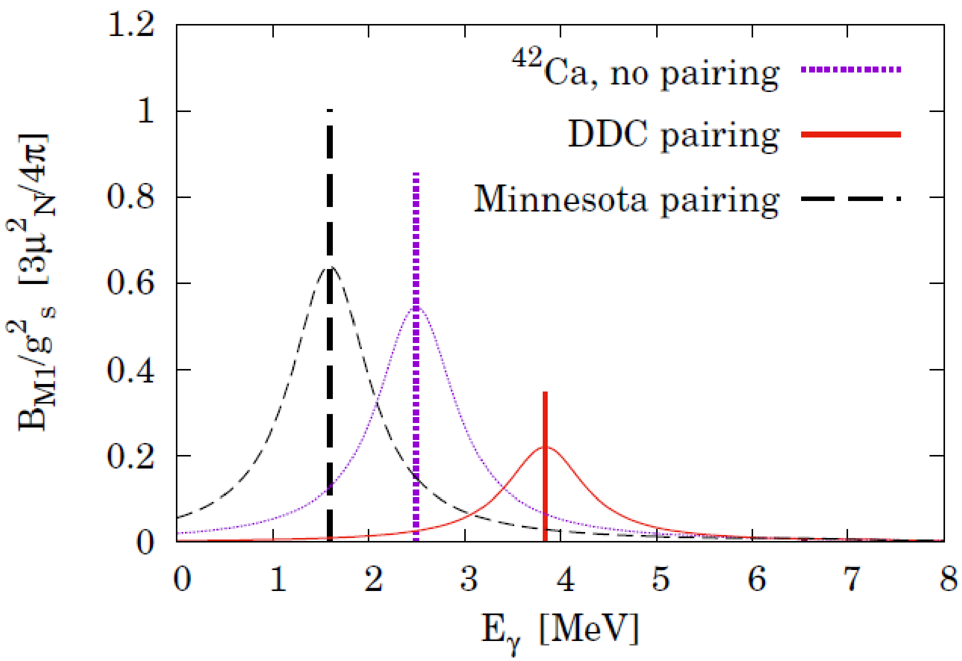

Search for the S_{12}=1 pairs of neutrons/protons(T_{12}=1)

S_{12}=0

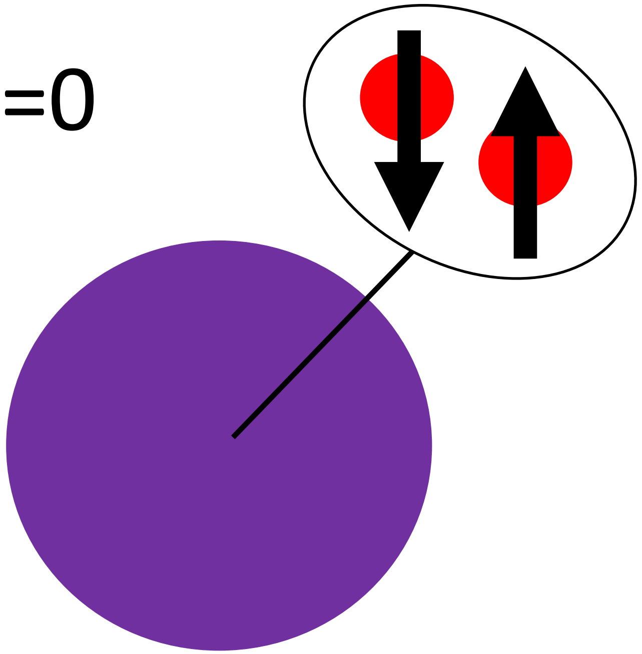

OR/AND

?

S_{12}=1

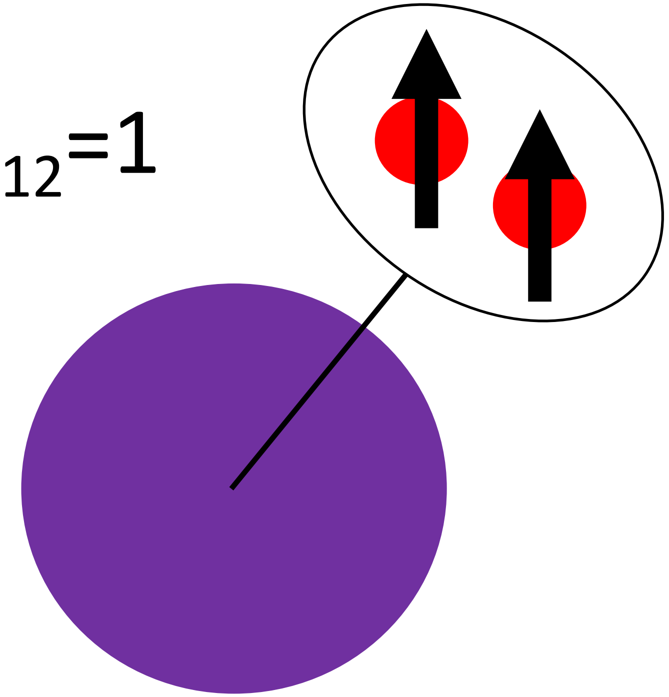

Like BCS coupling for electrons

Like Helium-3 superfluidity

Recent collaboration with K. Yoshida and N. Hihohara

➔Even with the S_{12}=0 pairing force only, there can emerge a finite S_{12}=1 component.

[N. Hihohara, TO, K. Yoshida, arXiv: 2308.02617]

NN scat. in many channels

Ryozo Tamagaki, Prog. Theo. Phys. Vol. 44, 905-928 (1970): theoretical evaluation.

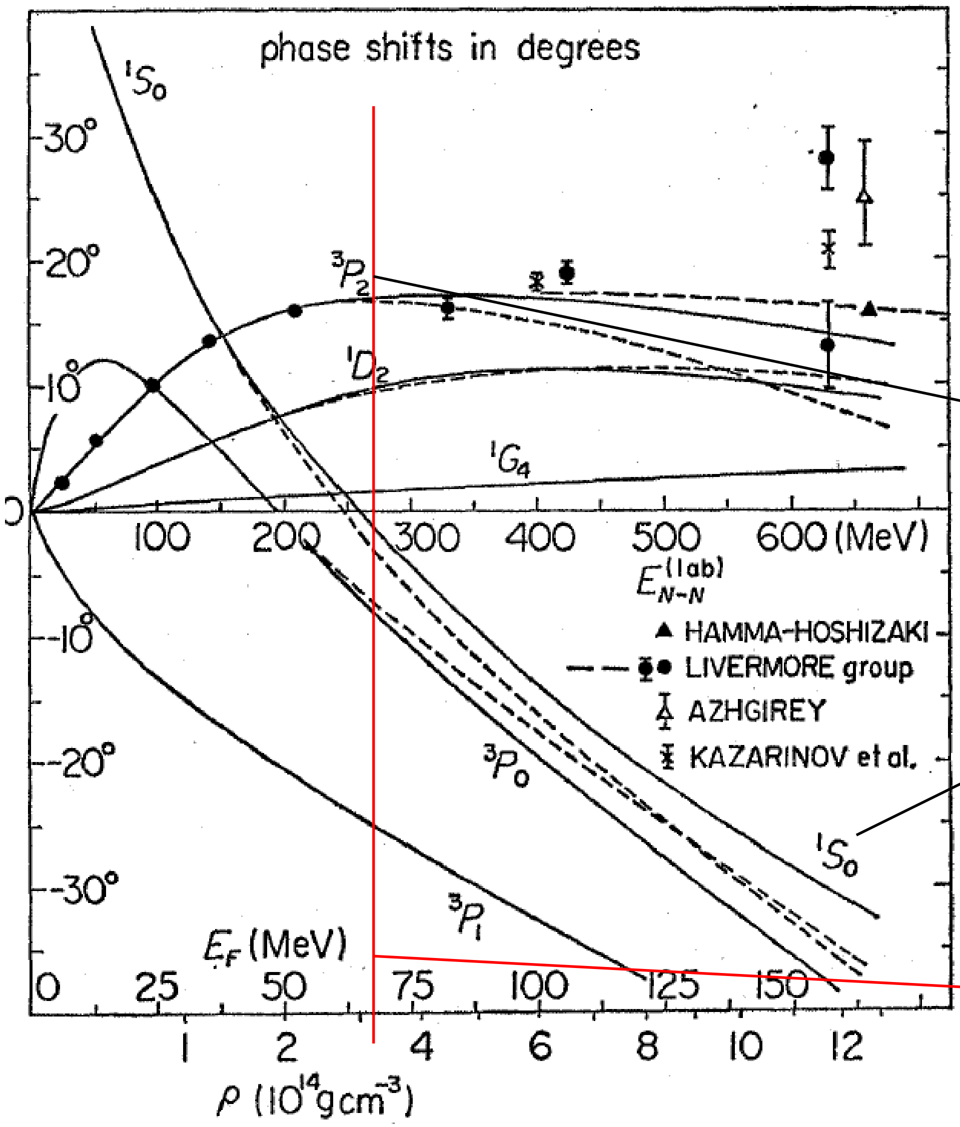

Fig. 1. Nucleon-nucleon scattering phase shifts versus $E_{N-N}^{(\mathrm{LAB})}=4E_F$. Solid (dotted) lines represent the phase shifts calculated from the OPEG potential with 2 GeV soft core (the OPEH potential with the hard core radius=0.42 fm).[9] For the $^3P_2$ phase shifts, solutions of the phase shift analysis are shown.[10]

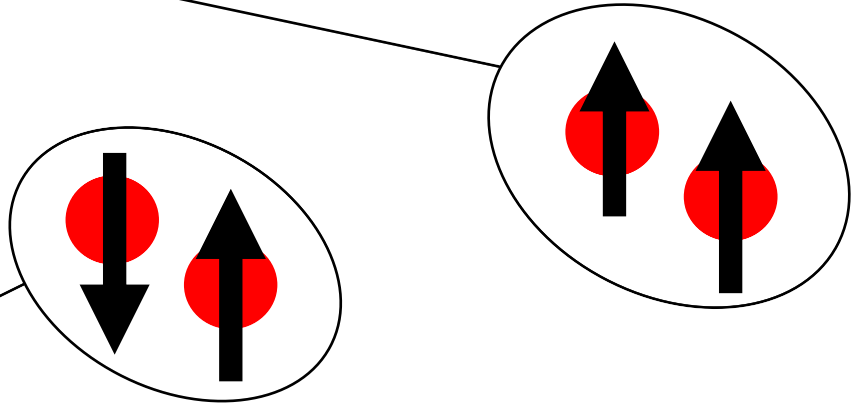

Normal density of nuclear matter:

$$\rho \cong 3.2\times 10^{14}\,\mathrm{g\,cm^{-3}}$$

Here I switch to the three-body model calculations for while…

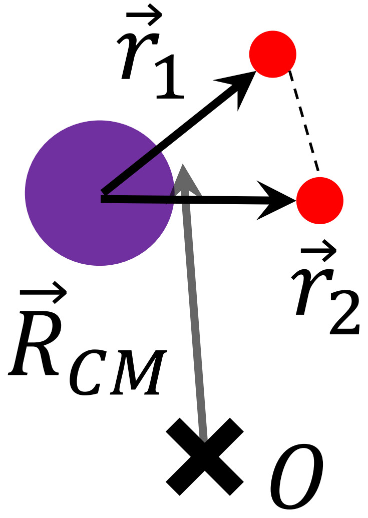

Three-body model: core + 2p

Y. Suzuki and K. Ikeda, Phys. Rev. C 38, 410 (1988).
G. Bertsch and H. Esbensen, Ann. Phys. 209, 327 (1991).

Two fermions (protons or neutrons) move around the core. ➔ Simple model of one nuclear (Cooper) pair inside the nucleus.

General coordinates:

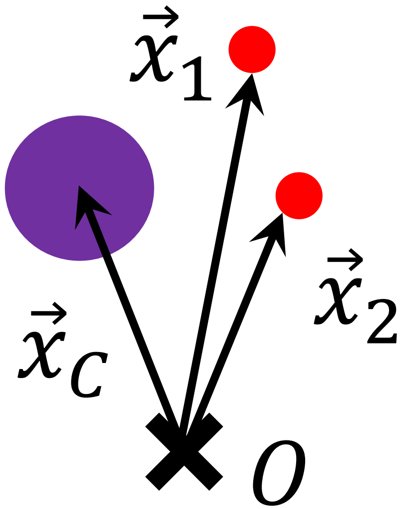

V + center-of-mass coordinates:

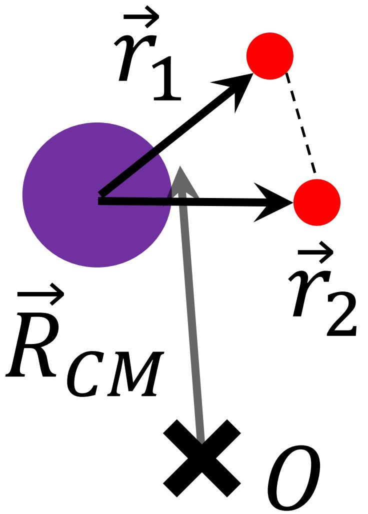

$$\begin{bmatrix} r_1 \\ r_2 \\ R_{CM} \end{bmatrix} = \begin{pmatrix} 1 & 0 & -1 \\ 0 & 1 & -1 \\ \frac{m_p}{M} & \frac{m_p}{M} & \frac{m_C}{M} \end{pmatrix} \begin{bmatrix} x_1 \\ x_2 \\ x_C \end{bmatrix}$$

$$\hat{H}_{3B} = -\frac{\hbar^2}{2m_p}\frac{\partial^2}{\partial x_1^2} - \frac{\hbar^2}{2m_p}\frac{\partial^2}{\partial x_2^2} - \frac{\hbar^2}{2m_C}\frac{\partial^2}{\partial x_C^2} + V(x_C, x_1) + V(x_C, x_2) + v_{pp}(x_1, x_2).$$

V = int. between core-p.
v_{pp} = int. between p-p.

$$\hat{H}_{3B} = \hat{h}(r_1) + \hat{h}(r_2) + v_{pp}(r_1, r_2) + \frac{p_1 \cdot p_2}{m_C} + \frac{P_{CM}^2}{2M}.$$

$$\hat{h}(r_i) = -\frac{\hbar^2}{2\mu}\frac{d^2}{dr_i^2} + \frac{\hbar^2}{2\mu}\frac{l(l+1)}{r_i^2} + V(r_i),$$

$$V(r_i) = V_{WS}(r_i) + V_{Coul}(r_i),$$

$\mu = m_p m_C/(m_p + m_C)$ and $m_p = 938.272$ MeV

Three-body model: core + 2p

Relation between jj-coupling (A) and LS-coupling (B) schemes of angular-momentum labels.

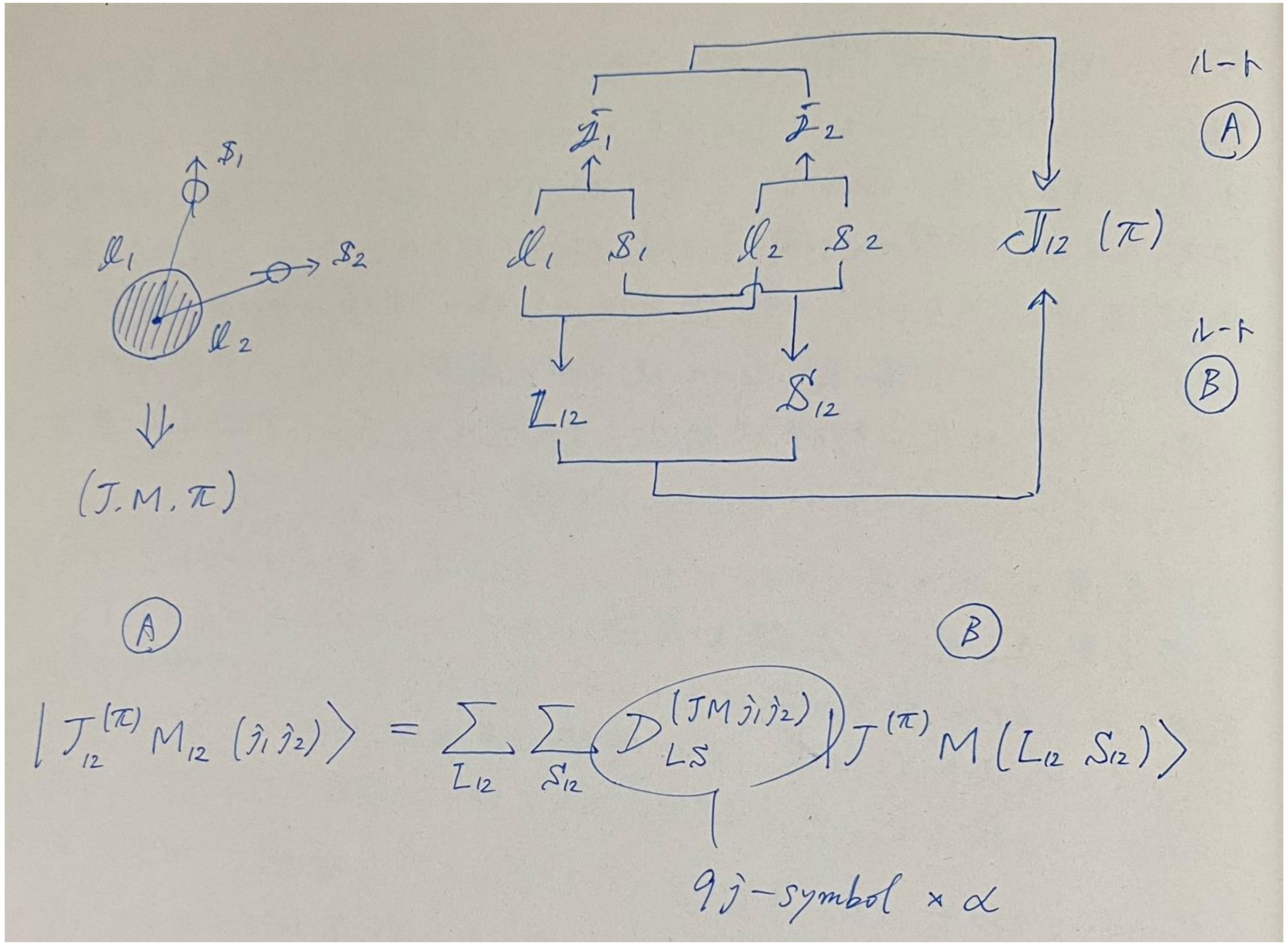

$$\vec{j}_1 = \vec{l}_1 + \vec{s}_1,$$
$$\vec{j}_2 = \vec{l}_2 + \vec{s}_2.$$

$$\vec{L}_{12} = \vec{l}_1 + \vec{l}_2,$$
$$\vec{S}_{12} = \vec{s}_1 + \vec{s}_2.$$

$$\Rightarrow \vec{J}_{12} = \vec{l}_1 + \vec{l}_2 + \vec{s}_1 + \vec{s}_2.$$

Potentials used in this three-body model

TO, N. Paar, PRC 100, 024308 (2019).

Hamiltonian:

$$\hat{H}_{3B} = \hat{h}(\boldsymbol{r}_1) + \hat{h}(\boldsymbol{r}_2) + v_{pp}(\boldsymbol{r}_1, \boldsymbol{r}_2) + \frac{\boldsymbol{p}_1 \cdot \boldsymbol{p}_2}{m_C} + \frac{\boldsymbol{P}_{CM}^2}{2M}.$$

$$\hat{h}(r_i) = -\frac{\hbar^2}{2\mu}\frac{d^2}{dr_i^2} + \frac{\hbar^2}{2\mu}\frac{l(l+1)}{r_i^2} + V(r_i),$$

$$V(r_i) = V_{WS}(r_i) + V_{Coul}(r_i),$$

Core-nucleon potential V(r) → energy levels of the core-nucleon subsystem.

Pairing force v_{pp} → fitted to the two-nucleon separation energy.

(1) Schematic density-dependent contact (DDC) interaction,

$$v_{NN}(\boldsymbol{r}_1, \boldsymbol{r}_2) = w(|\boldsymbol{R}_{12}|) \cdot \delta(\boldsymbol{r}_1 - \boldsymbol{r}_2),$$
$$w(r) = w_0 \left[1 - f(r)\right],$$

$$f(r) = \frac{1}{1 + e^{(r - R_0)/a_0}},$$

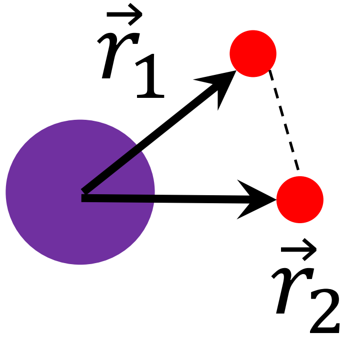

(2) Spin-dependent two-Gaussian interaction,

$$v_{NN}(\boldsymbol{r}_1, \boldsymbol{r}_2) = f \cdot U_{\rm MIN}(\boldsymbol{r}_1, \boldsymbol{r}_2)$$

$$U_{\rm MIN}(\boldsymbol{r}_1, \boldsymbol{r}_2) = v_r \exp\left(\frac{-d^2}{2q^2}\right) + v_s \exp\left(\frac{-d^2}{2\kappa_s^2 q^2}\right) \hat{P}_{S_{12}=0} + v_t \left(\frac{-d^2}{2\kappa_t^2 q^2}\right) \hat{P}_{S_{12}=1}$$

Wave functions solved in this three-body model

Hamiltonian:

$$\hat{H}_{3B} = \hat{h}(r_1) + \hat{h}(r_2) + \boxed{v_{pp}(r_1, r_2)} \boxed{+ \frac{p_1 \cdot p_2}{m_C}} + \frac{P_{CM}^2}{2M}.$$

$$\hat{h}(r_i) = -\frac{\hbar^2}{2\mu}\frac{d^2}{dr_i^2} + \frac{\hbar^2}{2\mu}\frac{l(l+1)}{r_i^2} + V(r_i),$$

$$V(r_i) = V_{WS}(r_i) + V_{Coul}(r_i),$$

Two-nucleon states = superposition of non-correlated basic states.

$$\langle r_1\sigma_1, r_2\sigma_2 \,|\, E_N \rangle = \sum_{ab} U_{N,ab} \tilde{\Phi}_{ab}(r_1\sigma_1, r_2\sigma_2),$$

$$\tilde{\Phi}_{ab}^{(JM,\pi)}(r_1\sigma_1, r_2\sigma_2) = \hat{A}\left[\phi_a(r_1\sigma_1) \otimes \phi_b(r_2\sigma_2)\right]^{(JM,\pi)},$$

$$\left[\hat{h}(r_1) + \hat{h}(r_2)\right] \tilde{\Phi}_{ab}^{(JM,\pi)} = (e_a + e_b)\, \tilde{\Phi}_{ab}^{(JM,\pi)}.$$

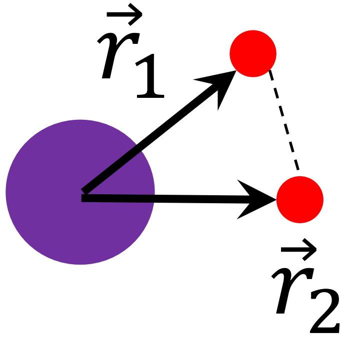

Expansion coefficients are obtained by diagonalizing non-diagonal terms.

Summation of M1 excitation of "one Cooper pair"

TO, N. Paar, PRC 100, 024308 (2019).

$$S_{\mathrm{M1}} \equiv \sum_f \left(\left| \left\langle f \middle| \hat{Q}_0 \middle| i \right\rangle \right|^2 + \left| \left\langle f \middle| \hat{Q}_+ \middle| i \right\rangle \right|^2 + \left| \left\langle f \middle| \hat{Q}_- \middle| i \right\rangle \right|^2 \right)$$

When only 2 nucleons can be active for M1,

$$\hat{Q}_{M1} = g_s[\hat{s}_1 + \hat{s}_2] + g_l[\hat{l}_1 + \hat{l}_2]$$

$$S_{\mathrm{M1}} = \left\langle i \middle| \left(g_l \hat{\mathbf{L}}_{12} + g_s \hat{\mathbf{S}}_{12} \right)^2 \middle| i \right\rangle$$
$$= (g_l^2 - g_l g_s) \left\langle \hat{\mathbf{L}}_{12}^2 \right\rangle^{(i)} + (g_s^2 - g_l g_s) \left\langle \hat{\mathbf{S}}_{12}^2 \right\rangle^{(i)}$$
$$+ g_l g_s \left\langle \hat{\mathbf{J}}^2 \right\rangle^{(i)},$$

Note: we discuss the M1 strength up to the one-body-operator level in this work.

When 2p/2n are coupled to $J^P=0^+$ at the initial state, possible combinations of (L_{12}, S_{12}) = (1,1) or (0,0) only. Thus,

$$S_{\mathrm{M1}}(J_i = 0) = 2(g_l - g_s)^2 \underbrace{N^{(i)}_{(L_{12}=1, S_{12}=1)}}_{\text{Spin-triplet ratio}}$$

Summation of $B_{M1}(E_f)$ coincides the spin-triplet (S_{12}=1) ratio in the initial state.

→ M1 transition can be used to infer the spin-triplet pairing ratio.

→ This spin-triplet ratio depends on the (l_1,l_2,j_1,j_2) labels combined with pairing v_{pp}.

Results for ^{42}Ca = ^{40}Ca + 2n

^{40}Ca core (mostly M1 silent)

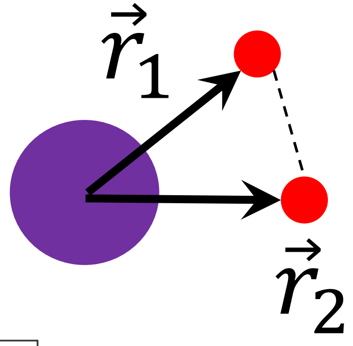

Note: E_{GS}= $-S_{2n}$= -19.843 MeV in experimental data.

- SRV = $g^2_s\ 2N_{S=1}$, VS,
- naive summation: $S_{\mathrm{M1,cal.}} = \sum_{E_\gamma} B_{\mathrm{M1}}(E_\gamma)$

	DDC	Minnesota	No pair.
E_{GS}	-19.232 MeV	-19.843 MeV	-16.795 MeV
$\langle v_{NN} \rangle$	-2.999 MeV	-3.221 MeV	0 MeV
$\langle x_{\mathrm{rec}} \rangle$	-0.005 MeV	-0.012 MeV	0 MeV
$N_{S_{12}=1}$	17.6% (numerical)	50.6% (numerical)	42.9% (analytic)
SRV	$0.352g_s^2$	$1.012g_s^2$	$0.858g_s^2$
$E_f^{(1)}$	-15.389 MeV	-18.253 MeV	-14.299 MeV
$S_{\mathrm{M1,cal.}}$	$0.352g_s^2$	$1.011g_s^2$	$0.857g_s^2$

$B_{M1}(E_\gamma;\ 0+ \rightarrow 1+)$, $E_\gamma = E_f - E_{GS}$

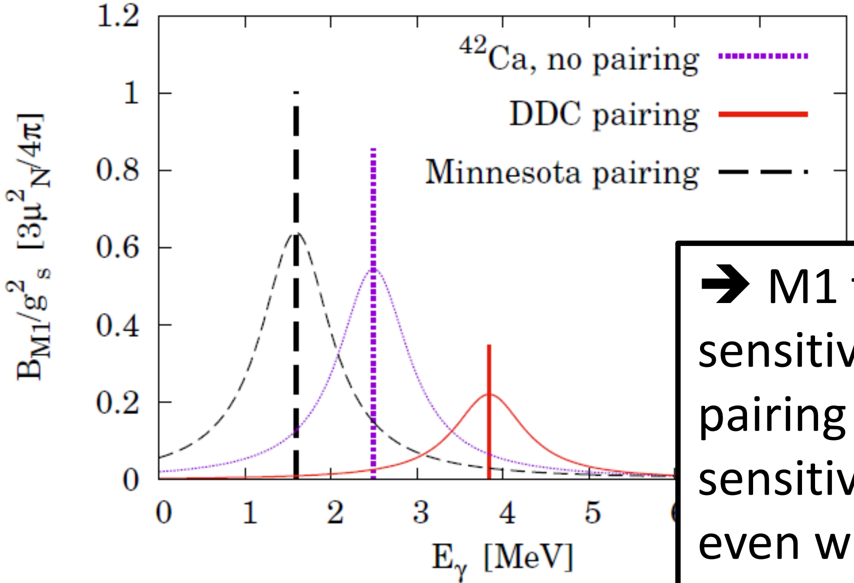

➔ M1 transition is sensitive to the pairing models. This sensitivity remains even when those are equivalently fitted to the same GS energy.

Two pairing-force models are used and compared. They reproduce the same energy.

DDC = density-dep. contact:

$$v_{NN}(\boldsymbol{r}_1, \boldsymbol{r}_2) = w(|\boldsymbol{R}_{12}|) \cdot \delta(\boldsymbol{r}_1 - \boldsymbol{r}_2),$$

$$w(r) = w_0 \left[1 - f(r)\right], \quad f(r) = \frac{1}{1 + e^{(r-R_0)/a_0}},$$

Minnesota = spin-dep. Gaussian:

$$v_{NN}(\boldsymbol{r}_1, \boldsymbol{r}_2) = f \cdot U_{\mathrm{MIN}}(\boldsymbol{r}_1, \boldsymbol{r}_2)$$

$$U_{\mathrm{MIN}}(\boldsymbol{r}_1, \boldsymbol{r}_2) = v_r \exp\left(\frac{-d^2}{2q^2}\right) + v_s \exp\left(\frac{-d^2}{2\kappa_s^2 q^2}\right) \hat{P}_{S_{12}=0} + v_t \left(\frac{-d^2}{2\kappa_t^2 q^2}\right) \hat{P}_{S_{12}=1}$$

Results of M1 in ^{18}O/ ^{18}Ne = ^{16}O + 2n/2p

TO, N. Paar, PRC 100, 024308 (2019).

^{18}O, E_{GS}(Exp.)= -12.188 MeV

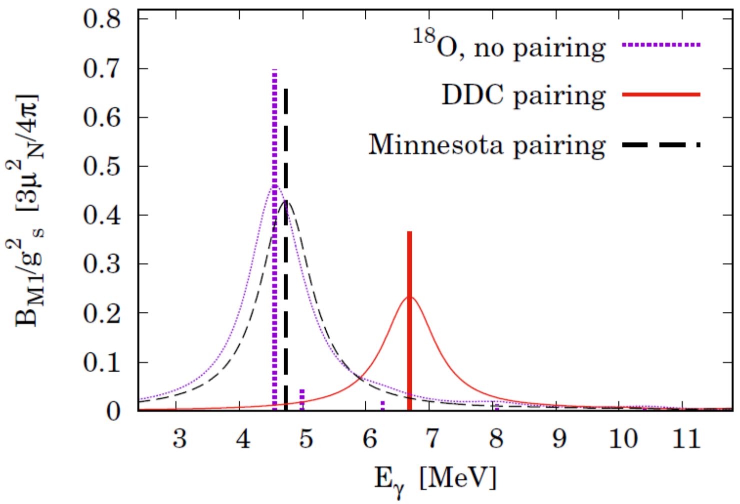

	DDC (full)	Minnesota	No pair.
E_{GS}	−12.019 MeV	−12.013 MeV	−8.286 MeV
$\langle v_{NN} \rangle$	−4.337 MeV	−4.022 MeV	0 MeV
$\langle x_{rec} \rangle$	−0.177 MeV	−0.404 MeV	0 MeV
$N_{d_{5/2} \otimes d_{5/2}}$	89.9%	94.9%	100%
$N_{S_{12}=1}$	19.7%	34.9%	40%
	(numerical)	(numerical)	(analytic)
SRV	$0.394 g_s^2$	$0.698 g_s^2$	$0.8 g_s^2$
$E_f^{(1)}$	−5.329 MeV	−7.286 MeV	−3.729 MeV
$S_{M1,cal.}$	$0.393 g_s^2$	$0.696 g_s^2$	$0.799 g_s^2$

^{18}Ne, E_{GS}(Exp.)= -4.523 MeV

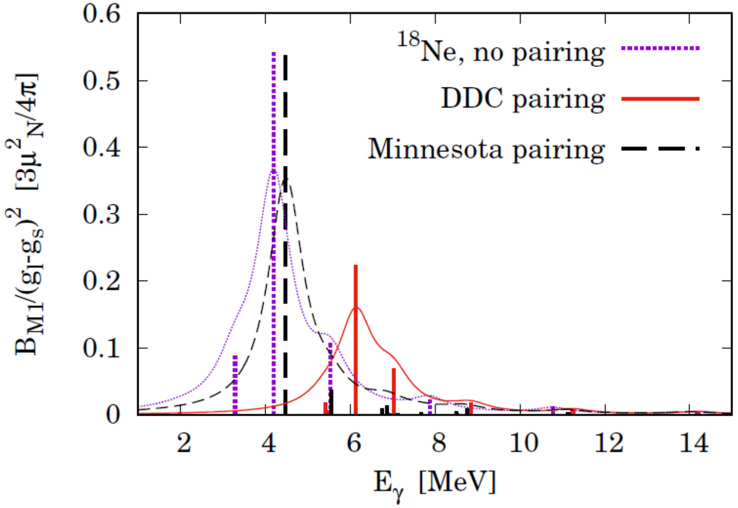

	DDC	Minnesota	No pair.
E_{GS}	−4.527 MeV	−4.524 MeV	−1.154 MeV
$\langle v_{pp} \rangle$	−4.015 MeV	−3.683 MeV	0 MeV
$\langle x_{rec} \rangle$	−0.127 MeV	−0.352 MeV	0 MeV
$N_{d_{5/2} \otimes d_{5/2}}$	88.5%	93.5%	100%
$N_{S_{12}=1}$	18.9%	33.0%	40%
	(numerical)	(numerical)	(analytic)
SRV	$0.378(g_l - g_s)^2$	$0.66(g_l - g_s)^2$	$0.8(g_l - g_s)^2$
$S_{M1,cal.}$	$0.376(g_l - g_s)^2$	$0.656(g_l - g_s)^2$	$0.799(g_l - g_s)^2$

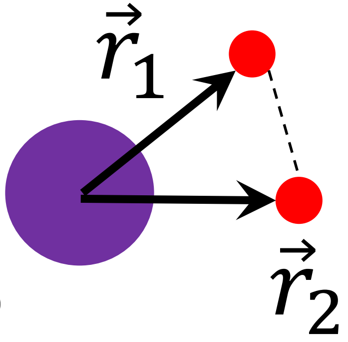

^{16}O
(mostly
M1 silent)

M1 excitation
⇔ S_{12}=1 pairing
ratio inside nuclei.

Now, let me return to the REDF-QRPA calculations.

$$\hat{\mathcal{H}}\left|\omega\right\rangle = E_{\omega}\left|\omega\right\rangle,$$

$$\left|\omega\right\rangle = \hat{\mathcal{Z}}^{\dagger}(\omega)\left|\Phi\right\rangle \qquad \hat{\mathcal{Z}}^{\dagger}(\omega) = \frac{1}{2}\sum_{\rho\neq\sigma}\left\{X_{\rho\sigma}(\omega)\hat{\mathcal{O}}^{(J,P)\dagger}_{\sigma\rho} - Y^{*}_{\rho\sigma}(\omega)\hat{\mathcal{O}}^{(J,P)}_{\sigma\rho}\right\},$$

$$\begin{pmatrix} A & B \\ B^{*} & A^{*} \end{pmatrix}\begin{pmatrix} X(\omega) \\ Y^{*}(\omega) \end{pmatrix} = \hbar\omega\begin{pmatrix} I & 0 \\ 0 & -I \end{pmatrix}\begin{pmatrix} X(\omega) \\ Y^{*}(\omega) \end{pmatrix},$$

Sensitivity of M1 to pairing models

Expt. = S. Bassauer et. al., Phys. Rev. C 102, 034327 (2020):

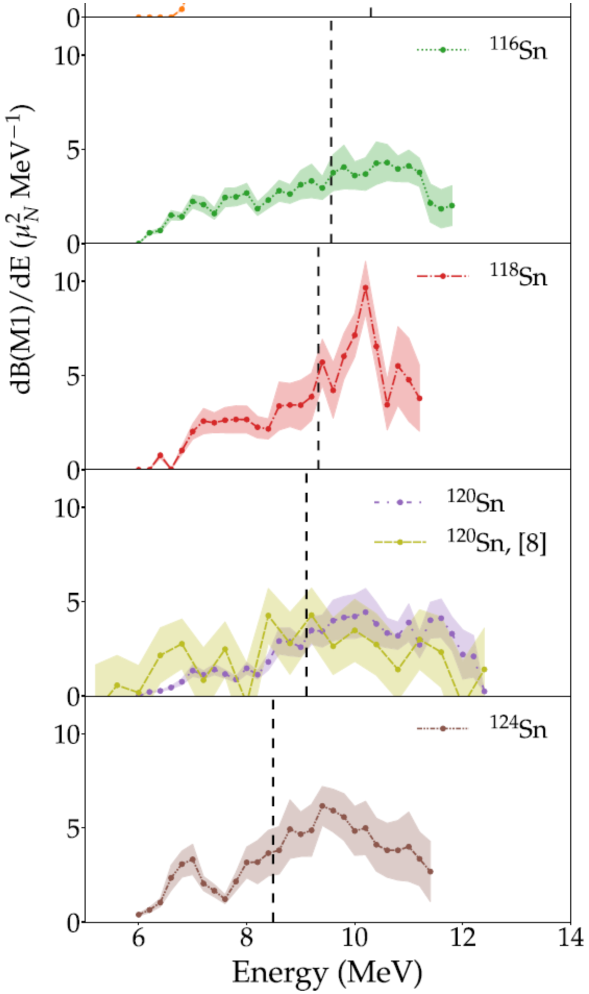

v.s. our QRPA results:

$$R_{\mathrm{M1}}(E) = \sum_{\nu} B_{\mathrm{M1}}(\omega_\nu) \frac{1}{\pi} \frac{\Gamma/2}{(E - \hbar\omega_\nu)^2 + (\Gamma/2)^2},$$

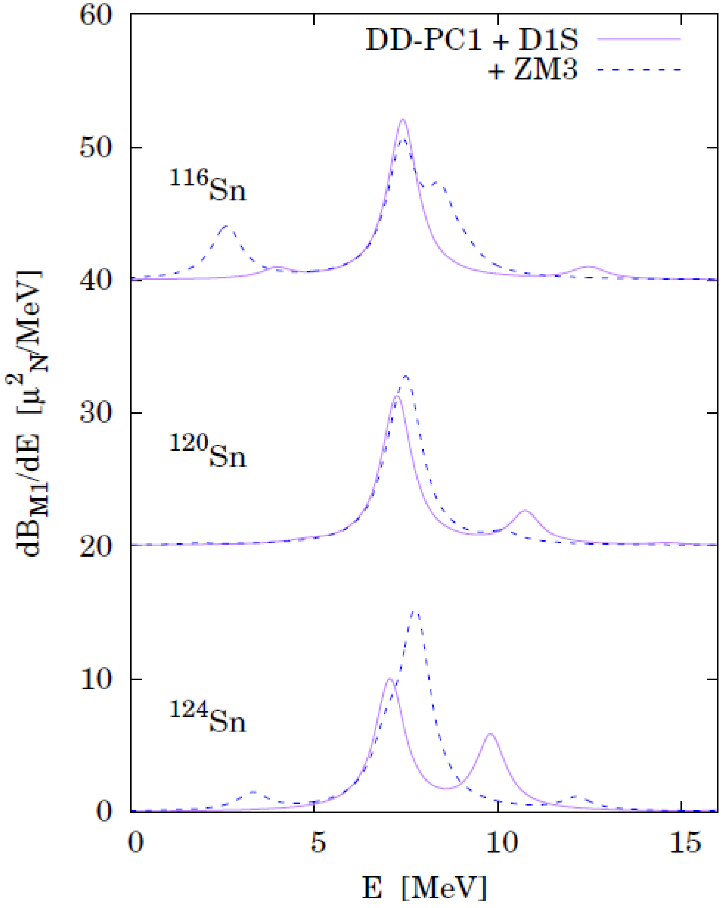

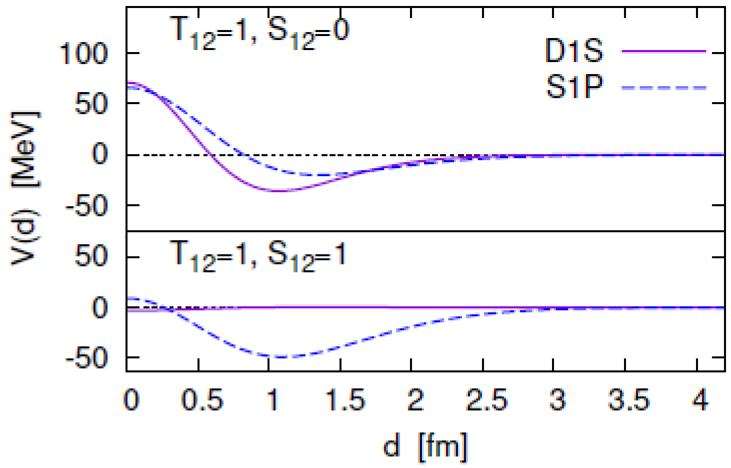

The major M1 energy is reproduced with both models. However, the ZM3(=S1P) predicts the low-lying peak, which is not measured.

➔ D1S looks better.

M1 excitations with rela’ mean-field + QRPA

TO, G Kruzic, N. Paar, Eur. Phys. J. A 57, 1-7 (2021).

RMF+QRPA results for M1 excitations with D1S (S_{12}=0) and S1P (S_{12}=1) pairing models.

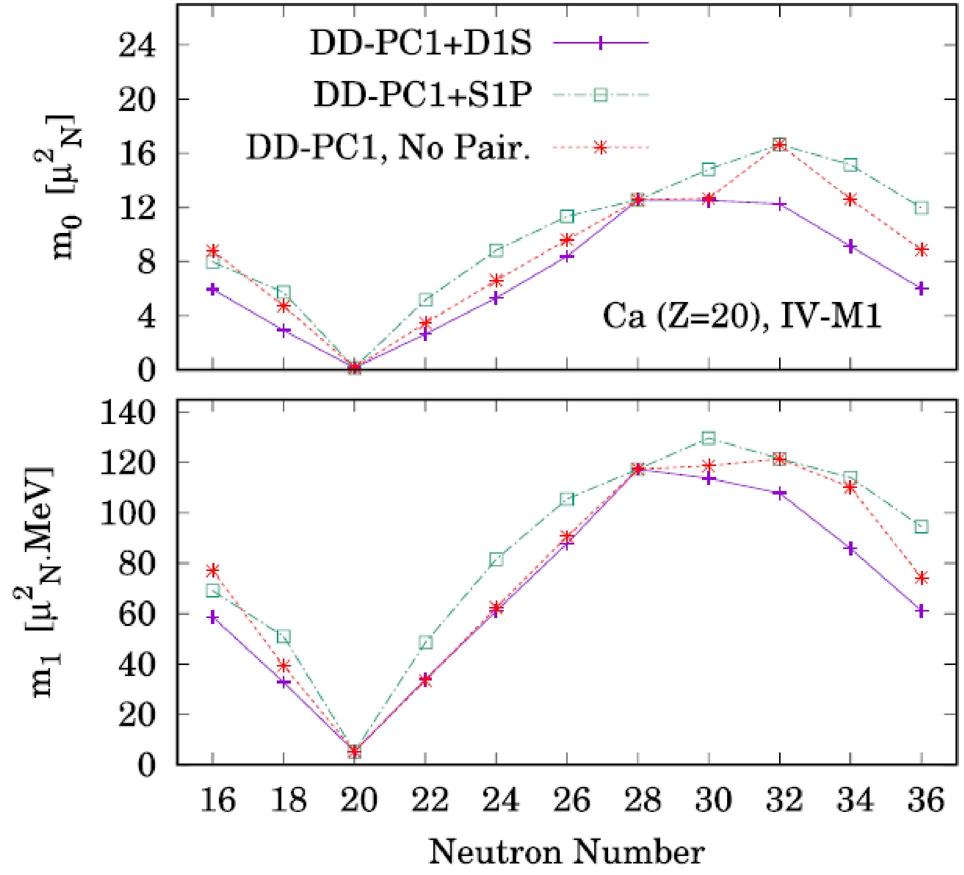

Fig. 4 (Top) Non-energy-weighted summation m_0 of the M1 strength in the DD-PC1 plus D1S pairing, +S1P pairing, and no pairing cases. (Bottom) Same but for the energy-weighted summation m_1

with

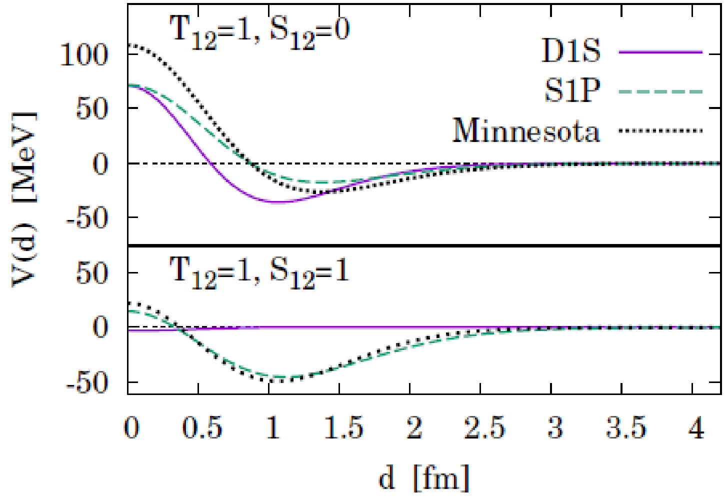

M1 summations across the close/open-shell isotopes remarkably depend on the nuclear Cooper-pair spin, S_{12}.

M1 excitations with rela' mean-field + QRPA

TO, G Kruzic, N. Paar, Eur. Phys. J. A 57, 1-7 (2021).

RMF+QRPA results for M1 excitations with D1S (S_{12}=0) and S1P (S_{12}=1) pairing models.

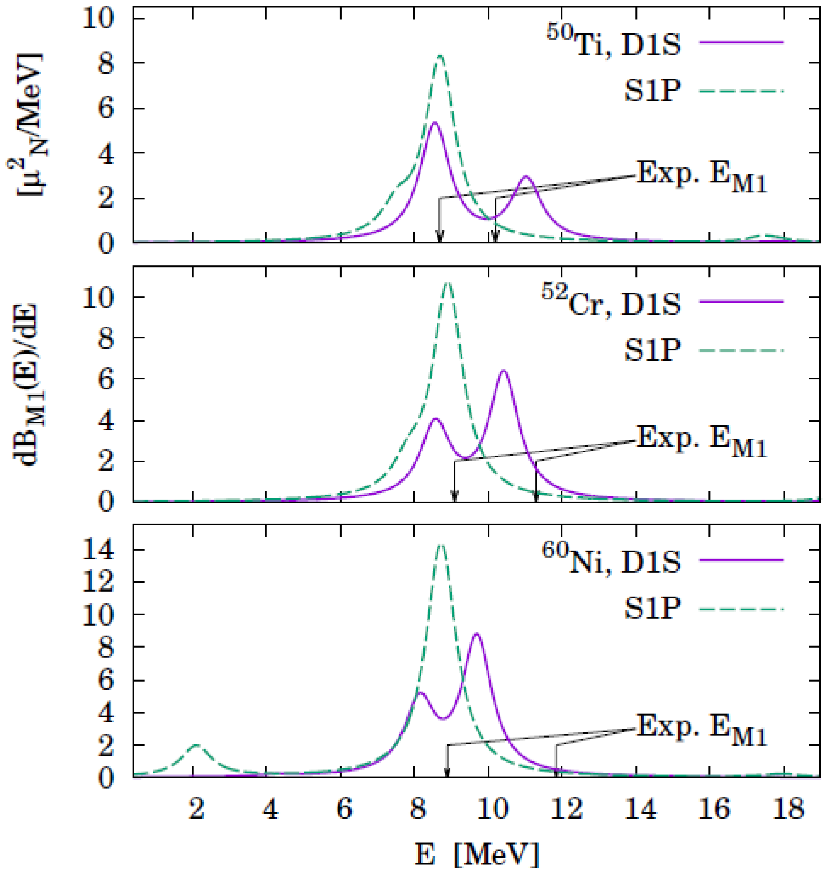

Expt. Data = D. I. Sober, et al, PRC 31, 2054 (1985)

with

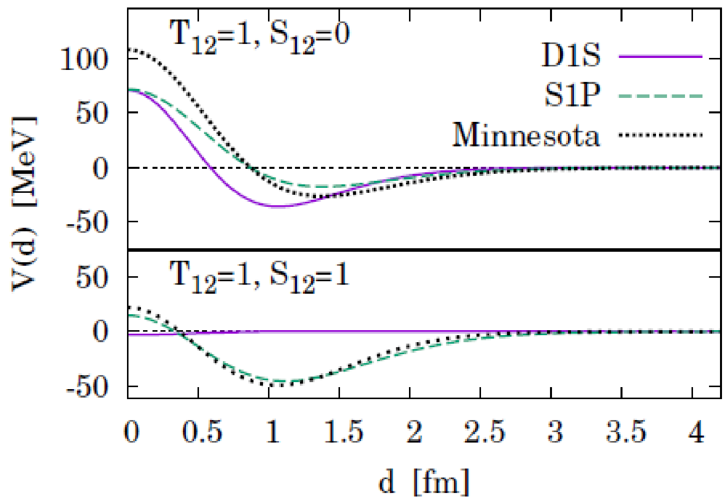

Conclusions from M1-with-pairing part:

- ✓ The "S_{12}=0 or 1" plays a role to control the M1 excitation energies and strengths.
- ✓ Systematic calculations of M1 may lead us to the finding of system(s) with large S_{12}=1 component.

Pair. Sensitivity of M1/M2/E1

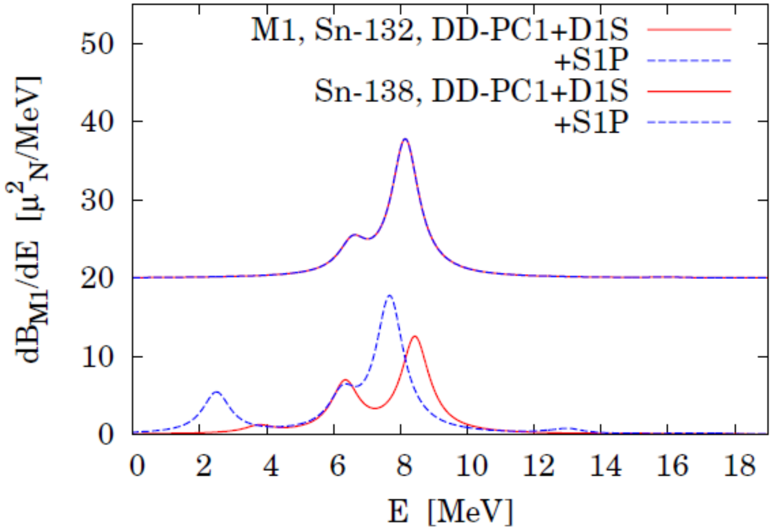

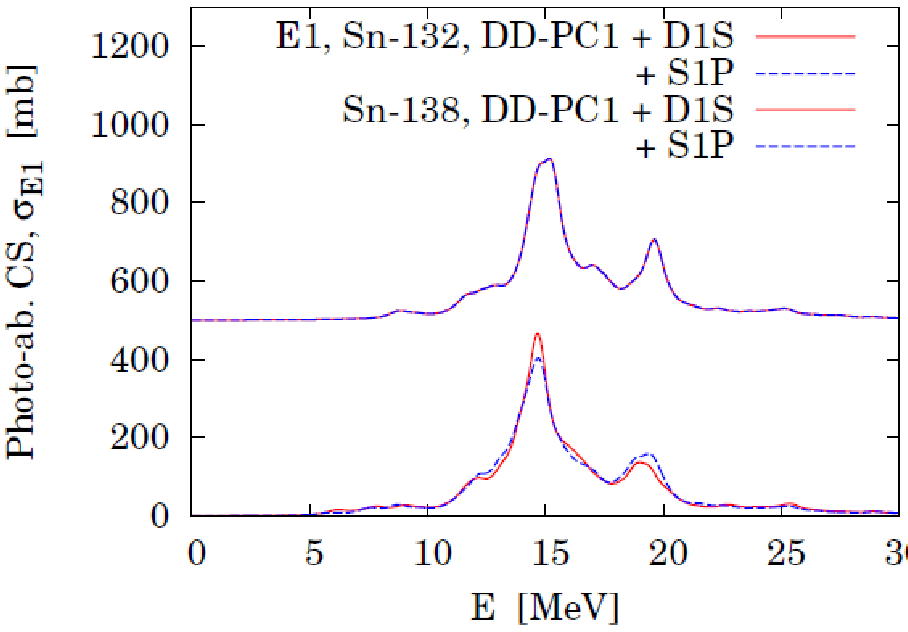

Test of QRPA in E1:

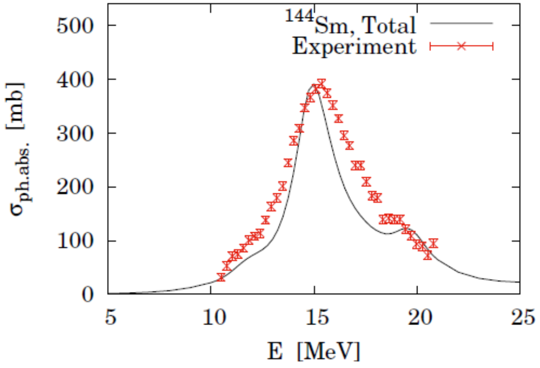

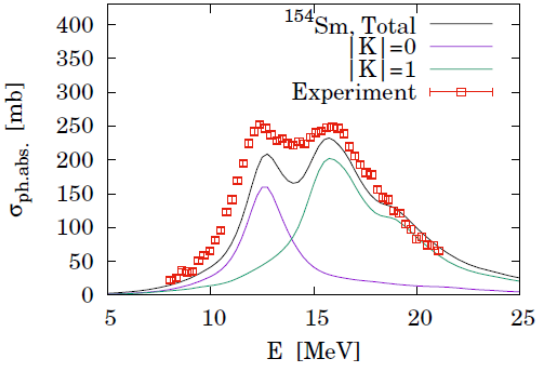

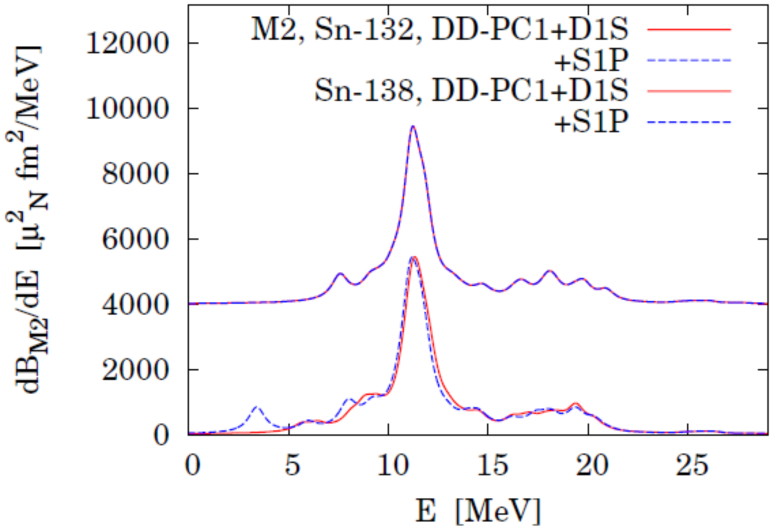

➔ M1 is especially sensitive to pairing modes.

➔ M2 with S1P yields the low-lying resonance.

➔ E1 is not sensitive. This insensitivity is checked also in E2 and E3.

Contents

Gamow-Teller (GT) and M1 transitions and their (broken) symmetry

Collaborators:
Nils Paar (Univ. of Zagreb, Croatia)
Ante Ravlic (Univ. of Zagreb, Croatia)
Goran Kruzic (Univ. of Zagreb & Ericsson-Nikola Tesla, Croatia)

Spin magnetic-dipole (M1) = spin-isospin mode A

The spin-M1 operator in its isovector (IV) mode contains the spin-isospin excitation operator.
Selection rule (even-even): 0+ ➔ 1+

$$\boxed{\hat{\mathcal{O}}^{\mathrm{M1}}_{\nu} = \sum_{k\in A} \hat{\tau}_0(k)\hat{s}_{\nu}(k),}$$

$$\hat{\mathcal{O}}^{\mathrm{GT}(\pm)}_{\nu} = \sum_{k\in A} \hat{\tau}_{\pm}(k)\hat{s}_{\nu}(k),$$

In M1 transitions, main contributions stem from the spin-orbit (SO) splitting as well as the relevant residual interactions.

$$\langle \mathcal{Y}_{l'j'} \mid\mid \hat{s} \mid\mid \mathcal{Y}_{lj} \rangle = \delta_{l'l}(-)^{l+j'+3/2}\sqrt{(2j'+1)(2j+1)} \begin{Bmatrix} 1/2 & j' & l \\ j & 1/2 & J=1 \end{Bmatrix} \cdot \sqrt{\frac{3}{2}}.$$

Only the $j_{>,<}$ ➔ $j_{<,>}$ transition is allowed.

The M1 mode also plays a role in the determination of neutron-capture rates, of significance for the r-process nucleosynthesis.

Gamow-Teller (GT) = spin-isospin mode B

Main component of charge-exchange reactions and beta-radioactivity. Its operator is similar to the M1, and the selection rule is the same but including the charge exchanging (CE).

$$\hat{\mathcal{O}}^{\mathrm{M1}}_{\nu} = \sum_{k \in A} \hat{\tau}_0(k) \hat{s}_{\nu}(k),$$

$$\boxed{\hat{\mathcal{O}}^{\mathrm{GT}(\pm)}_{\nu} = \sum_{k \in A} \hat{\tau}_{\pm}(k) \hat{s}_{\nu}(k),}$$

B(GT) 🡐 Two experimental probes have been utilized:

- Weak-interaction probe = beta radioactivity.
- Strong-interaction probe = CE reactions, e.g. by proton or ^{3}He scattering.

GT transitions 🡒 (i) nucleosynthesis, especially by determining the beta-decay lifetimes, which provide a key ingredient for understanding the r-process timescale; (ii) neutrino-induced reactions and electron capture in nuclei during the late stages of stellar evolution; (iii) double-beta decays(?).

M1 transition: link with neutrino-nuclear reaction

M1 matrix elements can be used to estimate the neutrino-nuclear reaction, which is important in astrophysical phenomena, e.g. r-process.
[K. Langanke et. al., PRL 93, 202501 (2004).]

$$\boldsymbol{O}(\mathrm{GT}_0) = \sum_k \boldsymbol{\sigma}(k)\boldsymbol{t}_0(k) = \sum_k 2\boldsymbol{s}(k)\boldsymbol{t}_0(k),$$

$$\boldsymbol{O}(M1)_{\mathrm{iv}} = \sqrt{\frac{3}{4\pi}}\sum_k[\boldsymbol{l}(k)\boldsymbol{t}_0(k) + (g_s^p - g_s^n)\boldsymbol{s}(k)\boldsymbol{t}_0(k)]\mu_N.$$

Neutrino-nuclear reaction:

$$\sigma_{i,f}(E_\nu) = \frac{G_F^2 g_A^2}{\pi(2J_i+1)}(E_\nu - \omega)^2 |\langle f || \sum_k \boldsymbol{\sigma}(k)\boldsymbol{t}(k) || i\rangle|^2,$$

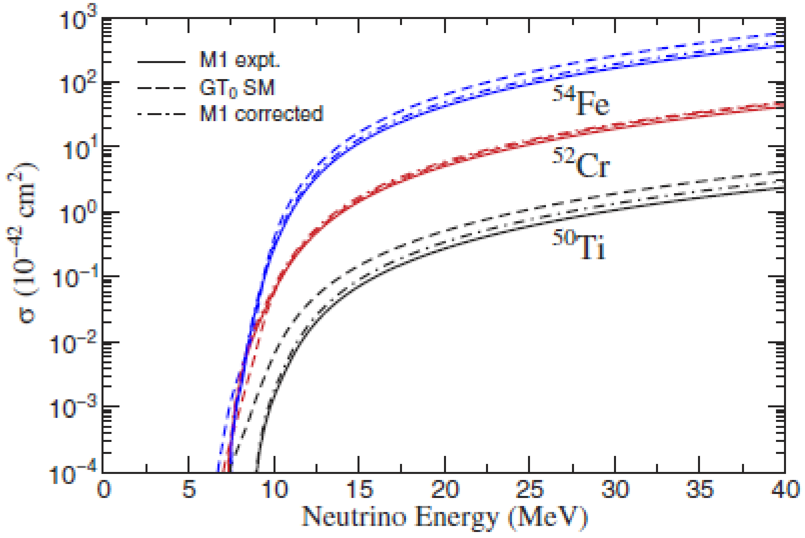

FIG. 2 (color online). Neutrino-nucleus cross sections, calculated from the $M1$ data (solid lines) and the shell-model (SM) GT_0 distributions (dashed lines) for ^{50}Ti (multiplied by 0.1), ^{52}Cr, and ^{54}Fe (times 10). The dash-dotted lines show the cross sections from the $M1$ data, corrected for possible strength outside the experimental energy window.

➔ The M1 M.E. can be common to the GT_0 M.E. for the neu.-nucl. reactions.

M1 and GT transitions

E.g. ^{42}Ca ~= ^{40}Ca+2n

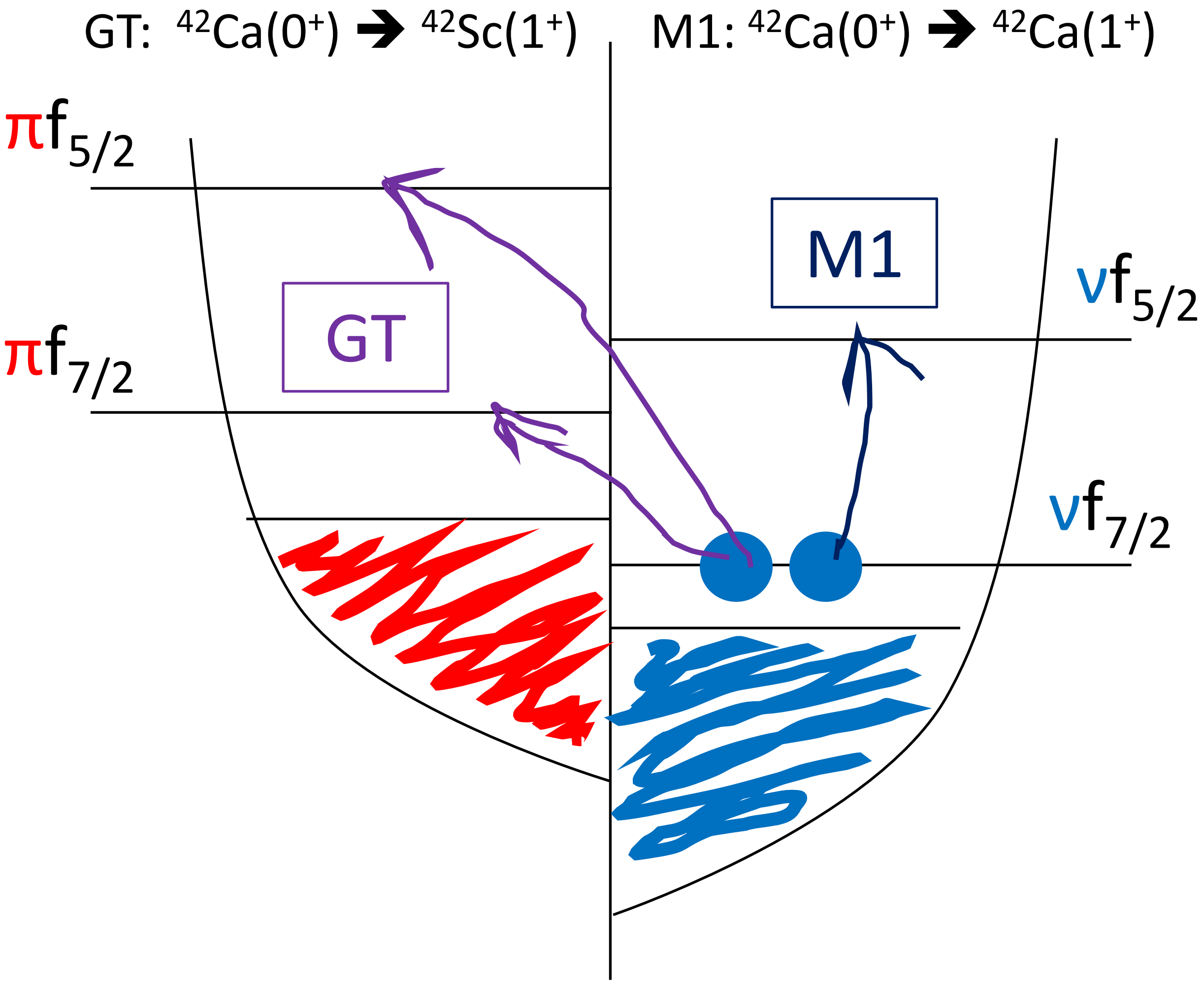

$$\hat{\mathcal{O}}_{\nu}^{\mathrm{M1}} = \sum_{k \in A} \hat{\tau}_0(k)\hat{s}_{\nu}(k),$$

$$\hat{\mathcal{O}}_{\nu}^{\mathrm{GT}(\pm)} = \sum_{k \in A} \hat{\tau}_{\pm}(k)\hat{s}_{\nu}(k),$$

E(M1) ~= E($\nu f_{5/2}$) - E($\nu f_{7/2}$), whereas ΔE(GT) ~= E($\pi f_{5/2}$) - E($\pi f_{7/2}$), with common selection rule: 0$^+$ ➔ 1$^+$.

M1 & GT can be interpreted as isobaric-analogue transitions. Does the theory reproduces them simultaneously? (LS splitting, res. interactions, pairing, etc.)

Model & methods (common to the previous ones)

- Relativistic Hartree-Bogoliubov (RHB) type with DD-PC REDFs.
- Relativistic quasi-particle random-phase approximation (QRPA) for M1/GT excitations.

$$\hat{\mathcal{H}}\,|\omega\rangle = \hbar\omega\,|\omega\rangle\,, \qquad |\omega\rangle = \hat{\mathcal{Z}}^{\dagger}(\omega)\,|\Phi\rangle\,, \quad \hat{\mathcal{Z}}^{\dagger}(\omega) = \frac{1}{2}\sum_{\rho\neq\sigma}\left\{X_{\rho\sigma}(\omega)\hat{\mathcal{Q}}^{\dagger}_{\sigma\rho} - Y^{*}_{\rho\sigma}(\omega)\hat{\mathcal{Q}}_{\sigma\rho}\right\},$$

$$\begin{pmatrix} A & B \\ B^{*} & A^{*} \end{pmatrix}\begin{pmatrix} X(\omega) \\ Y^{*}(\omega) \end{pmatrix} = \hbar\omega\begin{pmatrix} I & 0 \\ 0 & -I \end{pmatrix}\begin{pmatrix} X(\omega) \\ Y^{*}(\omega) \end{pmatrix}$$

$$\Rightarrow \quad R_X(E) = \sum_f \delta(E-E_f)B_X(E_f)$$

$$= \sum_f \delta(E-E_f)\sum_{\nu=\pm1,0}\left|\left\langle f\,\middle|\,\hat{\mathcal{O}}^{X}_{\nu}\,\middle|\,\Phi\right\rangle\right|^2$$

Point-Coupling REDF Lagrangian

In the relativistic nuclear theory (RNT), nucleon is described by a Dirac spinor $\psi(x)$, where $x = \{\boldsymbol{r}, \boldsymbol{s}, \vec{\tau}\}$. The phenomenological Lagrangian density reads

$$\mathcal{L} = \bar{\psi}(x)[i\gamma_\mu\partial^\mu - M]\psi(x) + \mathcal{L}_\mathrm{M} + \mathcal{L}_\mathrm{I}. \quad (1)$$

TABLE 2: Interaction terms included in $\mathcal{L}_\mathrm{I}$. Label (i) indicates isoscalar (IS) or isovector (IV). Label (ii) indicates scalar (S), vector (V), pseudo-scalar (PS) or pseudo-vector (PV).

(i)	(ii)	(T, J^π)	Meson	Meson-exchange	Point-coupling
IS	S	$(0, 0^+)$	σ	$-g_\sigma\bar{\psi}\sigma\psi$	$-\alpha_{\mathrm{IS-S}}(\rho)[\bar{\psi}\psi][\bar{\psi}\psi]/2$
					$-\delta_{\mathrm{IS-S}}(\rho)\partial_\mu[\bar{\psi}\psi]\partial^\mu[\bar{\psi}\psi]/2$
	V	$(0, 1^-)$	ω^μ	$-g_\omega[\bar{\psi}\gamma_\mu\omega^\mu\psi]$	$-\alpha_{\mathrm{IS-V}}(\rho)[\bar{\psi}\gamma_\mu\psi][\bar{\psi}\gamma^\mu\psi]/2$
	PS	$(0, 0^-)$	$\times$	$\times$	$\times$
	PV	$(0, 1^+)$	$\times$	$\times$	$\times$
IV	S	$(1, 0^+)$	$\times$	$\times$	$\times$
	V	$(1, 1^-)$	$\vec{\rho}^\mu$	$-g_\rho[\bar{\psi}\gamma_\mu(\vec{\tau}\vec{\rho}^\mu)\psi]$	$-\alpha_{\mathrm{IV-V}}(\rho)[\bar{\psi}\gamma_\mu\vec{\tau}\psi][\bar{\psi}\gamma^\mu\vec{\tau}\psi]/2$
	PS	$(1, 0^-)$	$\vec{\pi}$	$-ig_\pi[\bar{\psi}\gamma_5(\vec{\tau}\vec{\pi})\psi]$	$-\alpha_{\mathrm{IV-PS}}(\rho)[\bar{\psi}\gamma_5\vec{\tau}\psi][\bar{\psi}\gamma_5\vec{\tau}\psi]/2$
	PV	$(1, 1^+)$	$\partial_\mu\vec{\pi}$	$-\frac{f_\pi}{m_\pi}[\bar{\psi}\gamma_5\gamma_\mu\partial^\mu(\vec{\tau}\vec{\pi})\psi]$	$-\alpha_{\mathrm{IV-PV}}(\rho)[\bar{\psi}\gamma_5\gamma_\mu\vec{\tau}\psi][\bar{\psi}\gamma_5\gamma^\mu\vec{\tau}\psi]/2$
Coulomb					$-e\bar{\psi}\gamma_\mu A^\mu\left(\frac{1-\hat{\tau}_3}{2}\right)\psi$

In this work, we employ the point-coupling model.

Setting = DD-PC1 parameters.

Refs:
[1] T. Niksic, D. Vretenar, and P. Ring, Progress in Particle and Nuclear Physics 66(3), 519-548 (2011). [2] T. Niksic et. al., Comp. Phys. Communications, 107184 (2020).

Non-pertub. calculations for M1/GT transitions

$$R(E) = \sum_f \delta(E - E_f) \sum_{\nu=\pm 1,0} \left| \left\langle f \mid \hat{\mathcal{O}}_\nu^X \mid \Phi \right\rangle \right|^2$$

Non-perturbed calculations of REDF-based QRPA, where only the DD-PC1 Lagrangian is used.

- IV-PV ➔ Neglected.
- Pairing ➔ Neglected.

$$\hat{\mathcal{O}}_\nu^{\mathrm{IVM1}} = \cancel{g_s \mu_N \sqrt{\frac{3}{4\pi}}} \sum_{k\in A} \hat{\tau}_0(k)\hat{s}_\nu(k),$$

$$\hat{\mathcal{O}}_\nu^{\mathrm{GT}(\pm)} = \sum_{k\in A} \hat{\tau}_\mp(k)\hat{s}_\nu(k),$$

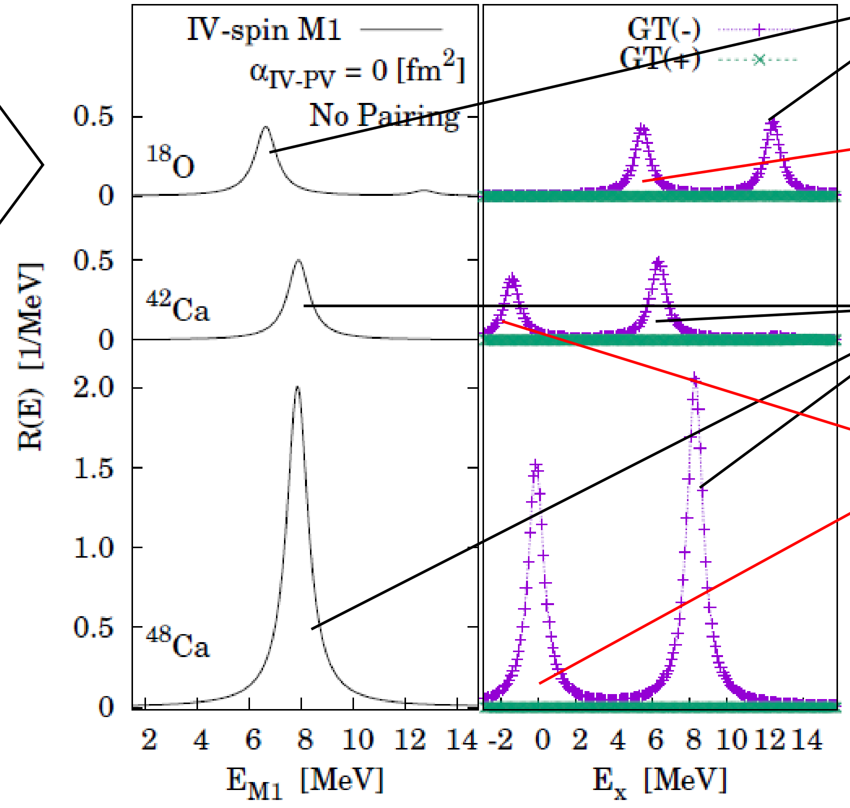

FIG. 1. Non-perturbed IV-spin M1 and GT(±) strength distributions obtained with RQRPA method, where residual interactions are neglected. The GT(±) energies E_x are presented with respect to the daughter nuclei.

$\nu(1d_{5/2}) \longrightarrow \nu(1d_{3/2})$ in IV M1, and
$\nu(1d_{5/2}) \longrightarrow \pi(1d_{3/2})$ in GT$(-)$,

$\nu(1d_{5/2}) \longrightarrow \pi(1d_{5/2})$ in GT$(-)$,

$\nu(1f_{7/2}) \longrightarrow \nu(1f_{5/2})$ in IV M1, and
$\nu(1f_{7/2}) \longrightarrow \pi(1f_{5/2})$ in GT$(-)$.

$\nu(1f_{7/2}) \longrightarrow \pi(1f_{7/2})$ in GT$(-)$.

- ✓ Equivalence between M1 and higher GT(-) is confirmed.
- ✓ GT(-) has another low-lying resonance.
- ✓ Ikeda-Fujita-Fujii SR for GT ➔ Checked.
- ✓ Kurath's SR for M1 ➔ Checked.

Next step = full REDF-QRPA with residual interactions

➔ Let’s see what happens when we add residual interactions.

(1) IV-PV: $\mathcal{L} = \mathcal{L}_{\mathrm{DD-PC1}} + \mathcal{L}_{\mathrm{IV-PV}}, \quad \mathcal{L}_{\mathrm{IV-PV}} = -\hbar c \frac{\alpha_{\mathrm{IV-PV}}}{2} \left[\bar{\psi}\gamma_5\gamma_\mu\vec{\tau}\psi\right] \left[\bar{\psi}\gamma_5\gamma^\mu\vec{\tau}\psi\right].$

(2) Paring for open-shell:

$$
\begin{aligned}
V_{\mathrm{pp,T0}}(d) &= \sum_{i=1,2} U_i(S_{12}) e^{-d^2/\mu_i^2} \\
V_{\mathrm{pp,T1}}(d) &= \sum_{i=1,2} V_i(S_{12}) e^{-d^2/\mu_i^2}, \text{ where } d = |\boldsymbol{r}_2 - \boldsymbol{r}_1|
\end{aligned}
$$

TABLE I. Interactions used in our RHB and RQRPA calculations. The label ph (pp) indicates the quasi-particle quasi-hole (quasi-particle quasi-particle) channel.

		M1	GT
RHB (0^+)	ph	DD-PC1	
	pp	T1 pairing	
RQRPA (1^+)	ph	DD-PC1 plus IV-PV	
	pp	T1 pairing	PN pairing

Full-REDF-QRPA results for M1 and GT transitions

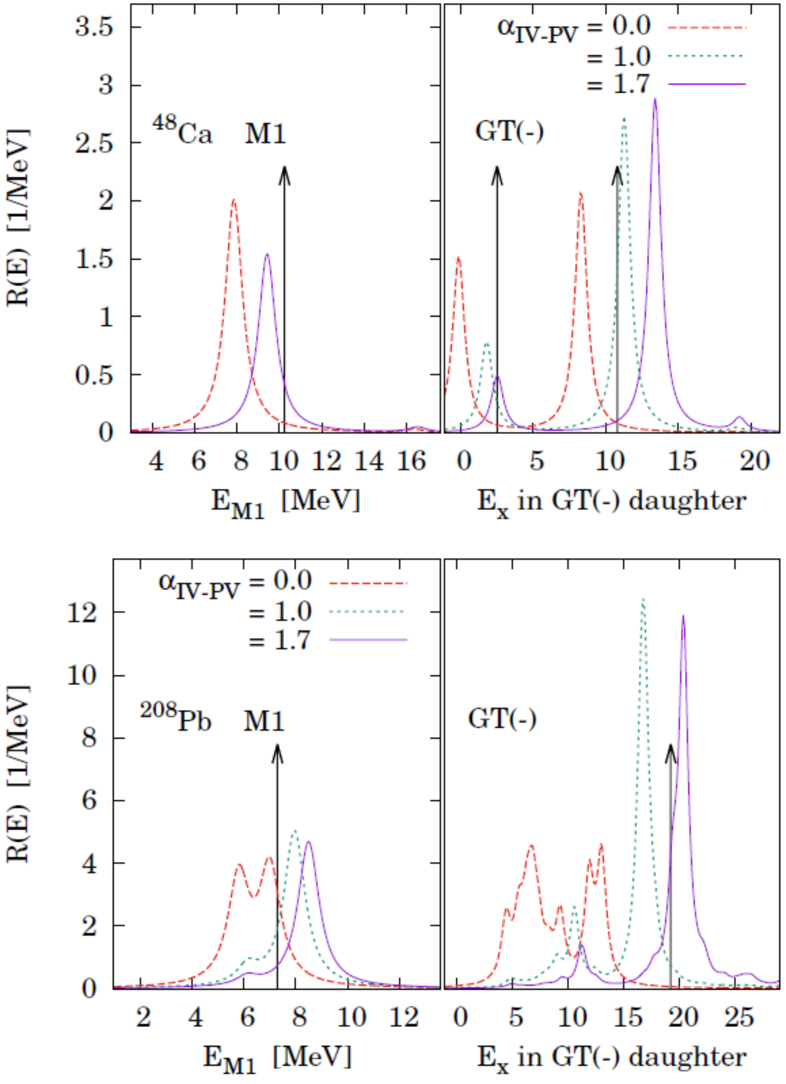

$$\mathcal{L}_{\mathrm{IV-PV}} = -\hbar c \frac{\alpha_{\mathrm{IV-PV}}}{2} \left[\bar{\psi}\gamma_5\gamma_\mu\vec{\tau}\psi\right] \left[\bar{\psi}\gamma_5\gamma^\mu\vec{\tau}\psi\right]$$

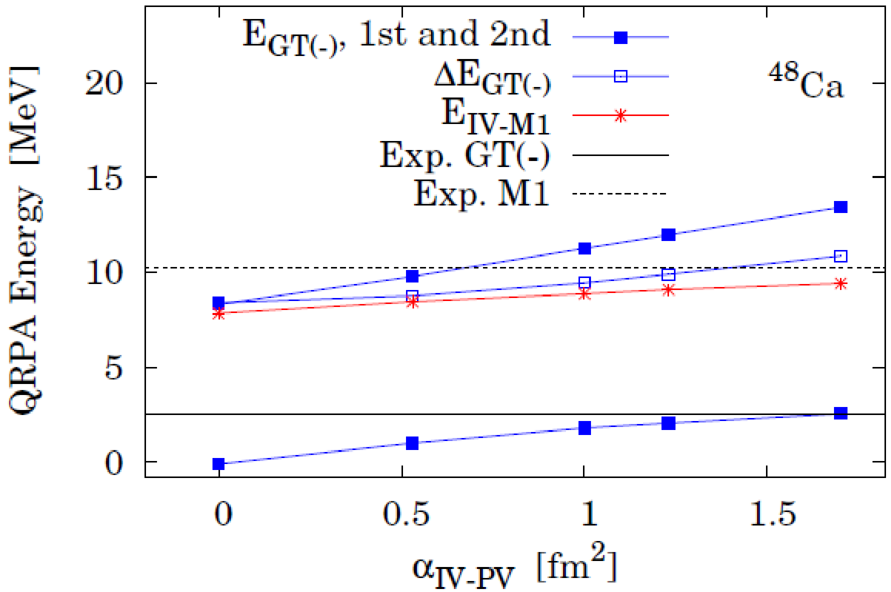

$$\hat{\mathcal{O}}^{\mathrm{IVM1}}_\nu = \cancel{g_s \mu_N \sqrt{\frac{3}{4\pi}}} \sum_{k\in A} \hat{\tau}_0(k)\hat{s}_\nu(k),$$

$$\hat{\mathcal{O}}^{\mathrm{GT}(\pm)}_\nu = \sum_{k\in A} \hat{\tau}_\mp(k)\hat{s}_\nu(k),$$

➔ As the residual IV-PV interaction becomes stronger, the M1 and GT modes become more divergent from each other. Namely, the IV-PV interaction disrupts the isobaric-analogue similarity between M1 and GT.

➔ Simultaneous reproduction of M1 & GT energies for both light and heavy nuclei is still demanding....

Mirror symmetry of M1 and GT transitions

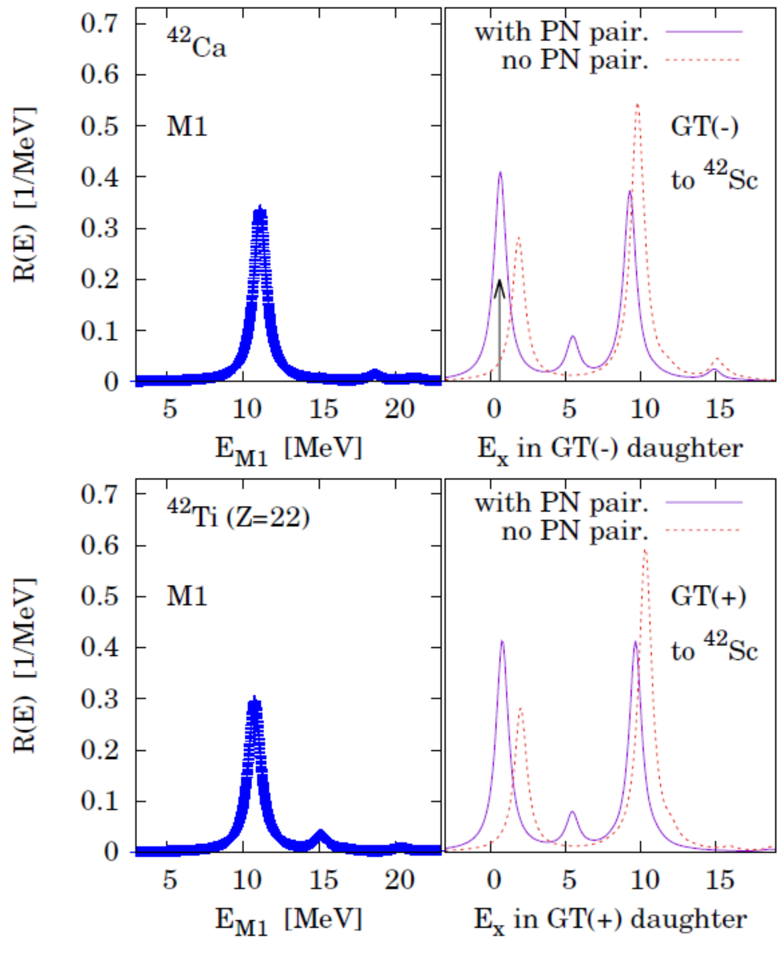

FIG. 5. The M1 and GT strength distributions of ^{42}Ca and ^{42}Ti. For GT($\pm$) modes, their excitation energies are presented with respect to the common daughter nucleus ^{42}Sc. The arrow indicates the experimental low-lying GT($-$) energy 0.611 MeV in ^{42}Sc [37].

"Colourful Nuclide Chart"

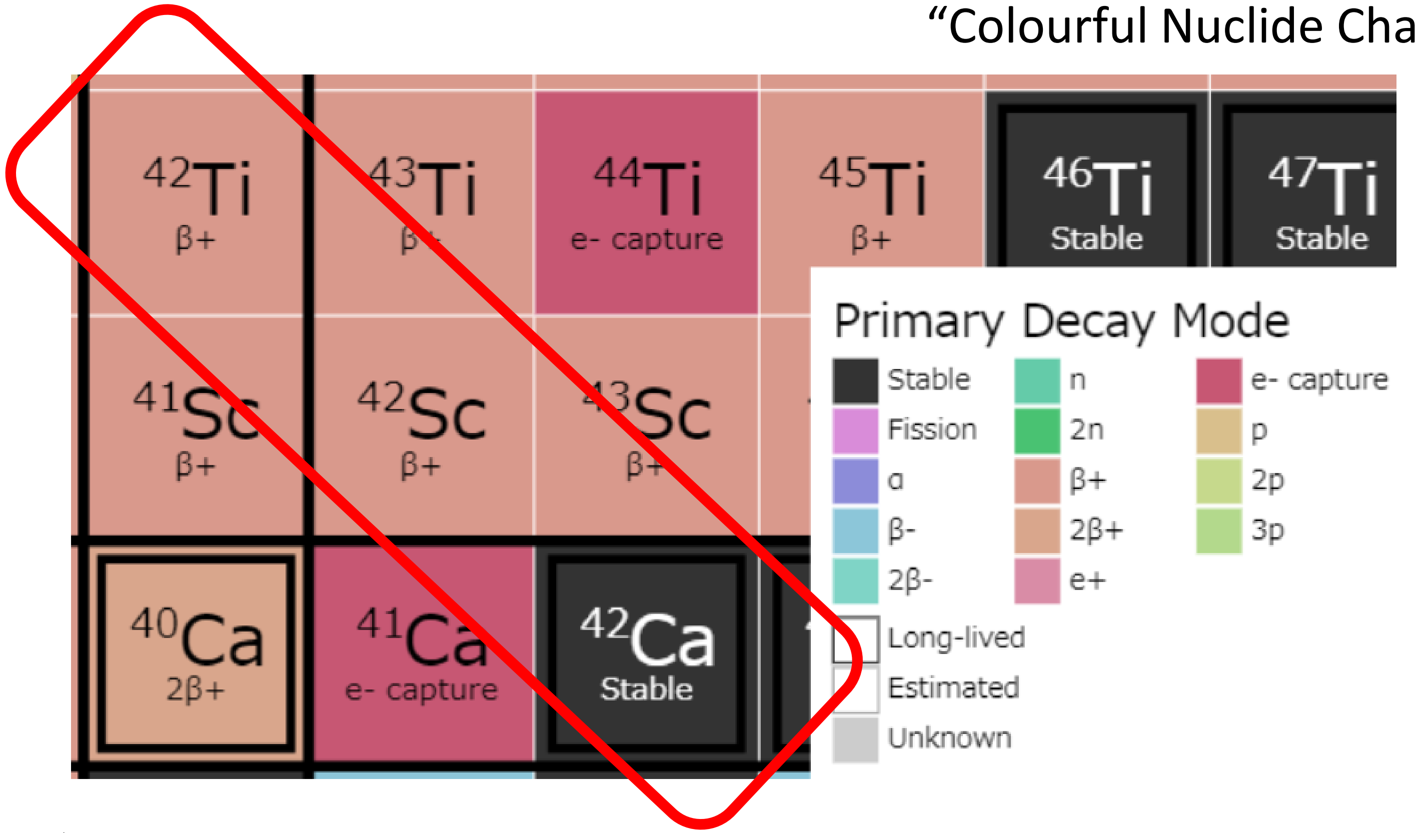

- ✓ Both M1 and GT(+)(-) transitions show an agreement between mirror-symmetric nuclei.

Mirror symmetry of M1 and GT transitions

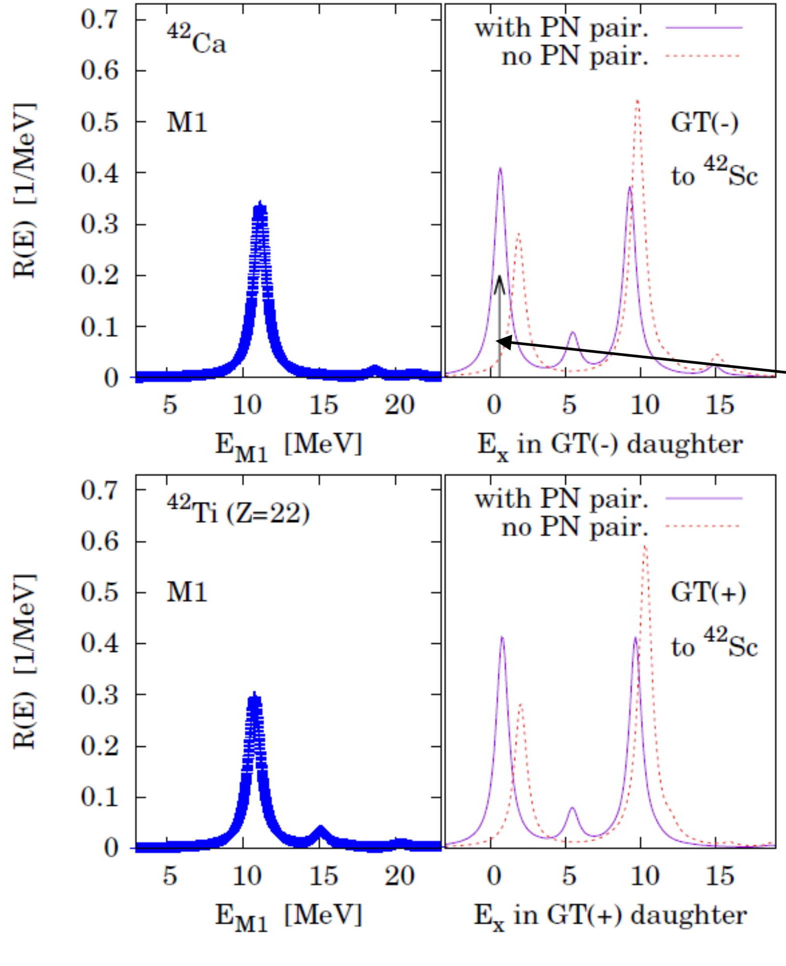

FIG. 5. The M1 and GT strength distributions of ^{42}Ca and ^{42}Ti. For GT($\pm$) modes, their excitation energies are presented with respect to the common daughter nucleus ^{42}Sc. The arrow indicates the experimental low-lying GT($-$) energy 0.611 MeV in ^{42}Sc [37].

Experimental data by Y. Fujita et al, Eur. Phys. J. A 56, 138 (2020): E_{GT} = 0.611 MeV.

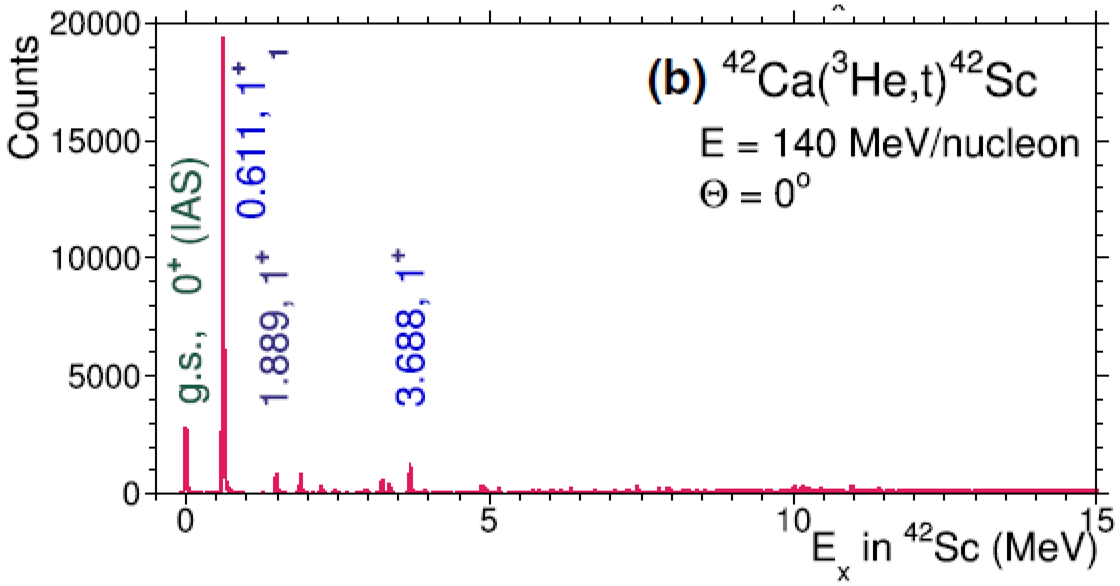

- ✓ Both M1 and GT(+)(-) transitions show an agreement between mirror-symmetric nuclei. Here pairing is taken into account.
- ✓ PN-pairing plays an essential role to explain the low-lying GT peaks.

Mirror symmetry of M1 and GT transitions

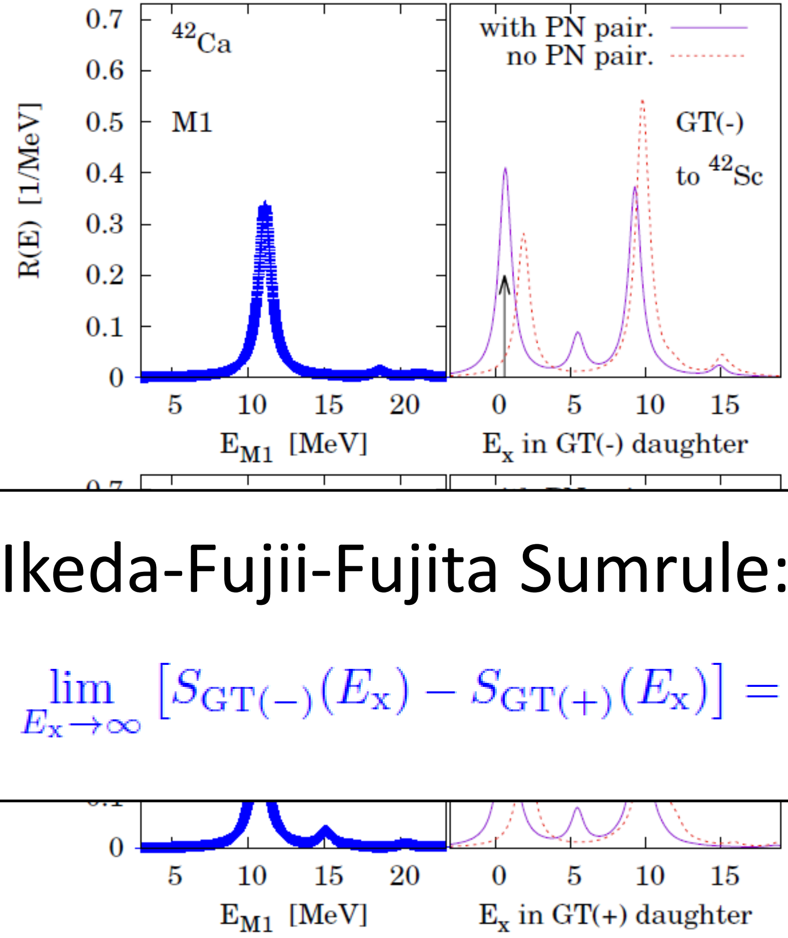

FIG. 5. The M1 and GT strength distributions of ^{42}Ca and ^{42}Ti. For GT($\pm$) modes, their excitation energies are presented with respect to the common daughter nucleus ^{42}Sc. The arrow indicates the experimental low-lying GT($-$) energy 0.611 MeV in ^{42}Sc [37].

Ikeda-Fujii-Fujita Sumrule:

$$\lim_{E_x \to \infty} \left[S_{\mathrm{GT}(-)}(E_x) - S_{\mathrm{GT}(+)}(E_x) \right] = \frac{3(N-Z)}{4},$$

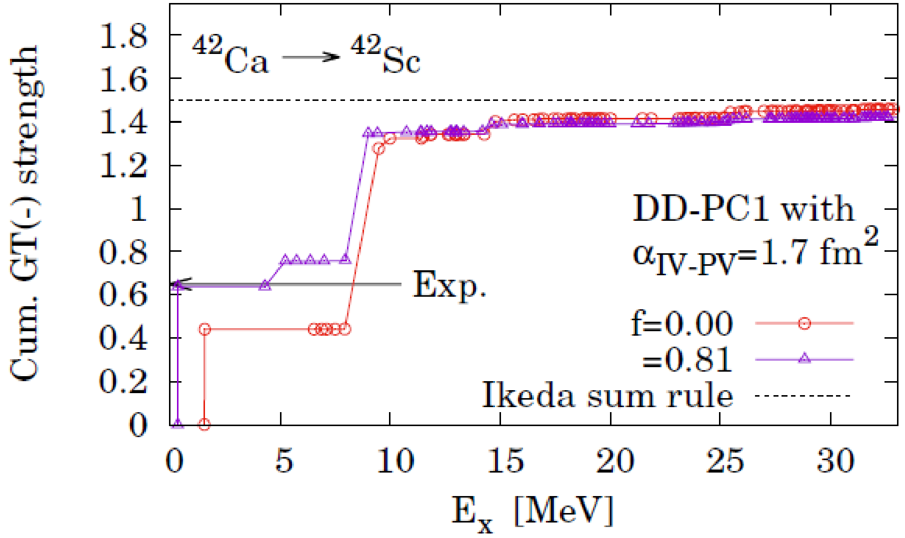

Figure 6. Cumulative GT($-$) strength for ^{42}Ca obtained with the DD-PC1 plus IV-PV interaction with $\alpha_{\mathrm{IV-PV}} = 1.7$ fm^2. Ikeda-Fujii-Fujita sum rule as in Eq. (14) is plotted by the dotted line. The arrow indicates the experimental value of $\sum B_{\mathrm{GT}(-)} = 2.6/4$ [55].

- ✓ Both M1 and GT(+)(-) transitions show an agreement between mirror-symmetric nuclei. Here pairing is taken into account.
- ✓ PN-pairing plays an essential role to explain the low-lying GT peaks.
- ✓ Giant GT somehow vanishes in experiments. Continuum effect?

Summary of GT/M1 part

The relativistic HB+QRPA computation is applied to the M1 and GT excitations.

- ✓ The IV-PV coupling remarkably affects the M1 and GT-excitation properties.
- ✓ For simultaneous reproduction of M1 and GT of various nuclei, we need to improve the REDF Lagrangian, e.g., with the density-dependent IV-PV couplings to reproduce the M1/GT energies of doubly-magic nuclei.
- ✓ The pairing interactions provide a sizable effect on these spin-isospin transitions. Especially the PN pairing is important to explain the low-lying GT excitations.

Contents

Relativistic QRPA for M2 excitation

Eur. Phys. J. A (2023) 59:50
https://doi.org/10.1140/epja/s10050-023-00958-0

THE EUROPEAN PHYSICAL JOURNAL A

Check for updates

Regular Article -Theoretical Physics

Magnetic quadrupole transitions in the relativistic energy density functional theory

Goran Kružić[1,a], **Tomohiro Oishi**[2,b], **Nils Paar**[3,c]

[1] Research Department, Ericsson-Nikola Tesla, Krapinska 45, 10000 Zagreb, Croatia
[2] Yukawa Institute for Theoretical Physics, Kyoto University, Kitashirakawa Oiwakechou, Sakyou, Kyoto, Japan
[3] Department of Physics, Faculty of Science, University of Zagreb, Bijenička c. 32, 10000 Zagreb, Croatia

Motivation

What we did before the M2↓

✓ Relativistic HB + QRPA for E1, M1, Gamow-Teller (GT), etc.

✓ Effect of residual interaction, pairing interaction, isobaric-analogue symmetry and its breaking, etc.

Why we choose the M2 as the next target?

✓ Indeed, M2 is minor, and could be less impacting than E1, M1, etc.

✓ However, we had one question: "Is the quenching factor fitted to M1 data can be valid in the M2 case, too?" → We still wait for data…

✓ Von-N. Cosel et. al. are now planning the systematic measurement of M2. Thus, nice data for reference will be possibly obtained near future.

QRPA for M2 excitation

M2-excitation strength:

$$B_{M2}(E_i) = \left|\beta_{M2}^{IS}(E_i) + \beta_{M2}^{IV}(E_i)\right|^2. \quad (8)$$

Here the IV-M2 amplitude is determined as

$$\beta_{M2}^{IV}(E_i) = \sum_{j_k j_{k'}} \left(X^i_{j_k j_{k'}} + (-1)^{j_k - j_{k'}} Y^i_{j_k j_{k'}}\right) \times \left(u_{j_k} v_{j_{k'}} + v_{j_k} u_{j_{k'}}\right) \langle j_{k'} || \hat{\mu}^{(IV)}_{\lambda=2} || j_k \rangle \tau_{IV}, \quad (9)$$

with $\tau_{IV} = 1\ (-1)$ for neutrons (protons). On the other side, the IS-M2 amplitude reads

$$\beta_{M2}^{(IS)}(E_i) = \sum_{j_k j_{k'}} \left(X^i_{j_k j_{k'}} + (-1)^{j_k - j_{k'}} Y^i_{j_k j_{k'}}\right) \times \underbrace{\left(u_{j_k} v_{j_{k'}} + v_{j_k} u_{j_{k'}}\right)} \langle j_{k'} || \hat{\mu}^{(IS)}_{\lambda=2} || j_k \rangle. \quad (10)$$

Those are solved from QRPA.

These were obtained with HB before QRPA.

with M2 operator:

$$\hat{\mu}^{(IS,IV)}_{\lambda\nu}(11)_k = \hat{\mu}^{(IS,IV)}_{\lambda\nu}(22)_k = \frac{\mu_N}{\hbar}\left(\frac{2}{\lambda+1} g_\ell^{(IS,IV)} \hat{\ell}_k + g_s^{(IS,IV)} \hat{s}_k\right) \nabla\left[r^\lambda Y_{\lambda\nu}(\Omega_k)\right]. \quad (5)$$

$$g_\ell^{IS} = \frac{g_\ell^\pi + g_\ell^\nu}{2} = 0.5, \quad g_s^{IS} = \frac{g_s^\pi + g_s^\nu}{2} = 0.880, \quad (6)$$

for the IS mode, whereas

$$g_\ell^{IV} = \frac{g_\ell^\pi - g_\ell^\nu}{2} = 0.5, \quad g_s^{IV} = \frac{g_s^\pi - g_s^\nu}{2} = 4.706, \quad (7)$$

for the IV mode.

Result: M2 strength in Ca-48 (1)

G. Kružić, TO, and N. Paar, Eur. Phys. Journal A 59(3), page 50 (2023).

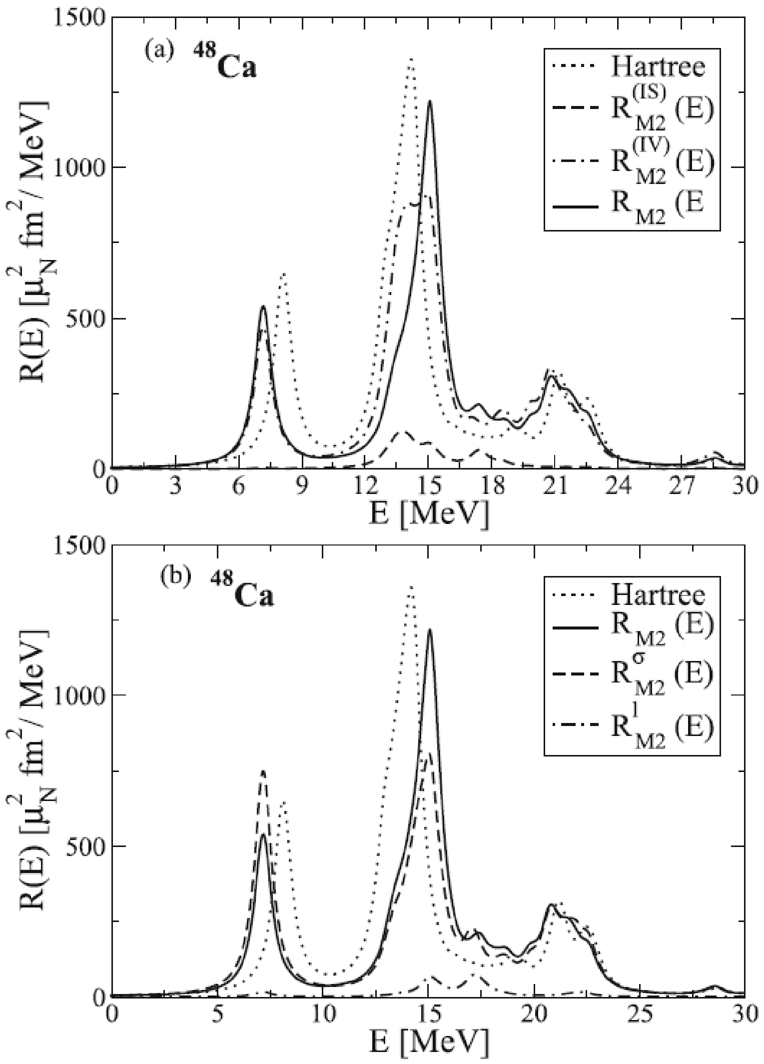

By taking the energy-weighted (EW) summation,

EW-M2 sum. (our model, up to 40 MeV.)

= 76.1 x 10^3 MeVμ^2_Nfm^2 for ^{48}Ca;

= 160.1 x 10^3 MeVμ^2_Nfm^2 for ^{90}Zr.

VS

(experimental data, up to 15 MeV.)

= 15.7 x 10^3 MeVμ^2_Nfm^2 for ^{48}Ca;

= 23.6 x 10^3 MeVμ^2_Nfm^2 for ^{90}Zr.

[P. von-N.-Cosel et. al., PRL 82, 1105 (1999).]

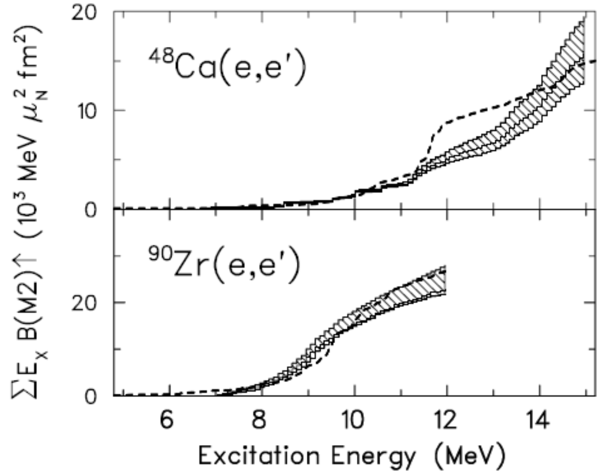

➔ If the high-energy M2 data will become available, the consistency may be restored.

Quenching effect in M1

G. Kruzic, T.O., N. Paar, PRC 103, 054306.

We performed the systematic evaluation of M1 in Sn isotopes:

Our REDF-QRPA result

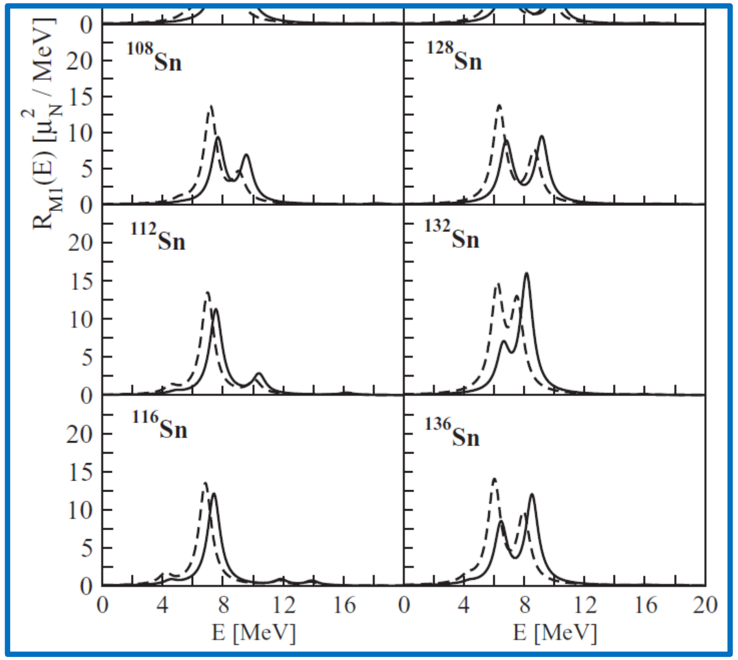

➔ Summation of M1 strength:

	$\sum B_{M1}^{th.}$	$\sum B_{M1}^{exp.}$	g_{eff}/g_{free}
^{112}Sn	22.81	14.7(1.4)	0.80
^{114}Sn	22.61	19.6(1.9)	0.93
^{116}Sn	22.56	15.6(1.3)	0.83
^{118}Sn	22.76	18.4(2.4)	0.89
^{120}Sn	23.34	15.4(1.4)	0.81
^{124}Sn	25.55	19.1(1.7)	0.86

Exp. Data from S. Basseur et. al., PRC 102, 034327 (2020).

✓ Quenching of 0.8-0.9 is necessary to reproduce the exp. M1 summation, i.e., it is not bad.

✓ Note that the experimental M1 distribution is quite broad, whereas our result is based on a narrow-resonance assumption.

Result: M2 strength in Ca-48 (2)

G. Kružić, TO, and N. Paar, Eur. Phys. Journal A 59(3), page 50 (2023).

Effect of residual IV-PV interaction: $$\mathcal{L}_{\mathrm{IV-PV}} = -\frac{1}{2}\alpha_{\mathrm{IV-PV}}[\bar{\Psi}_N\gamma^5\gamma^\mu\boldsymbol{\tau}\Psi_N][\bar{\Psi}_N\gamma^5\gamma_\mu\boldsymbol{\tau}\Psi_N].$$

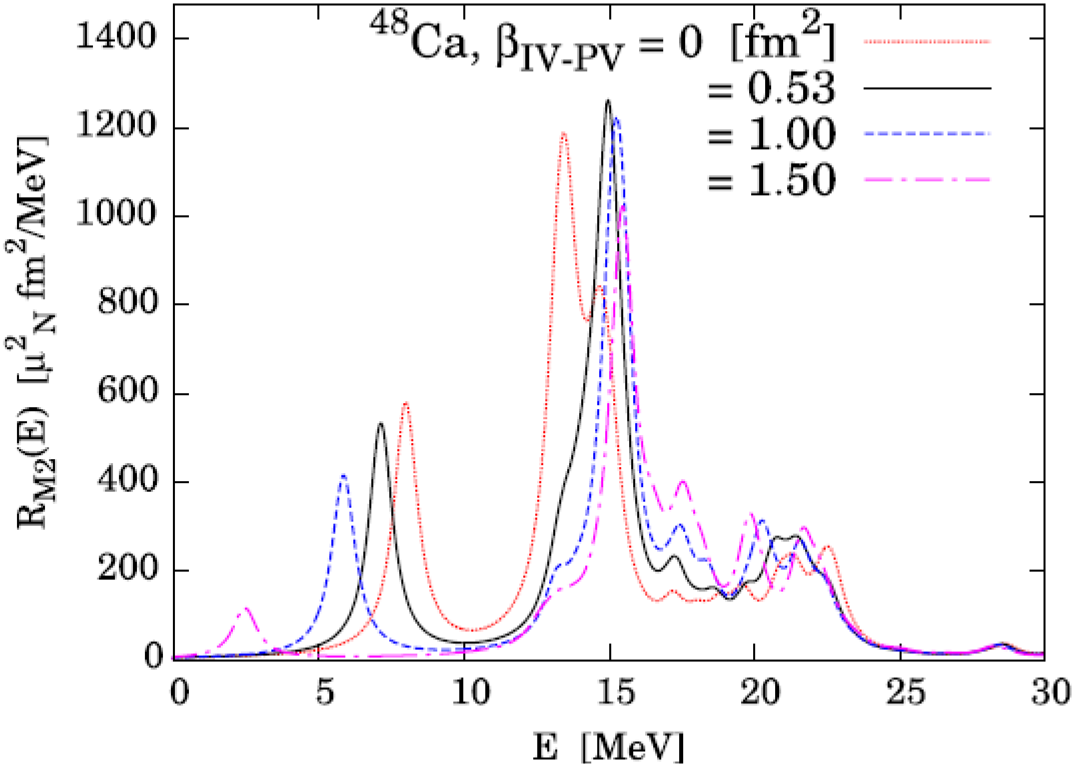

Fig. 3 The M2 transition strength distributions for ^{48}Ca by changing the IV-PV coupling strength parameter, $\alpha_{\mathrm{IV-TV}} = \beta_{\mathrm{IV-PV}} \cdot \hbar c$. Note that $\beta_{\mathrm{IV-TV}} = 0.53$ fm^2 is the default setting when combined with the DD-PC1 interaction

- ✓ The IV-PV interaction affects the M2 excitation from 0+ GS to 2- states.
- ✓ This effect was also confirmed in the M1 case. Energy shifts of M1 and M2 modes are in the same order, namely, a few MeV.
- ✓ Note that this shift did not affect the EW-M2 summation.

Result: M2 strength in Ca isotopes

G. Kružić, TO, and N. Paar, Eur. Phys. Journal A 59(3), page 50 (2023).

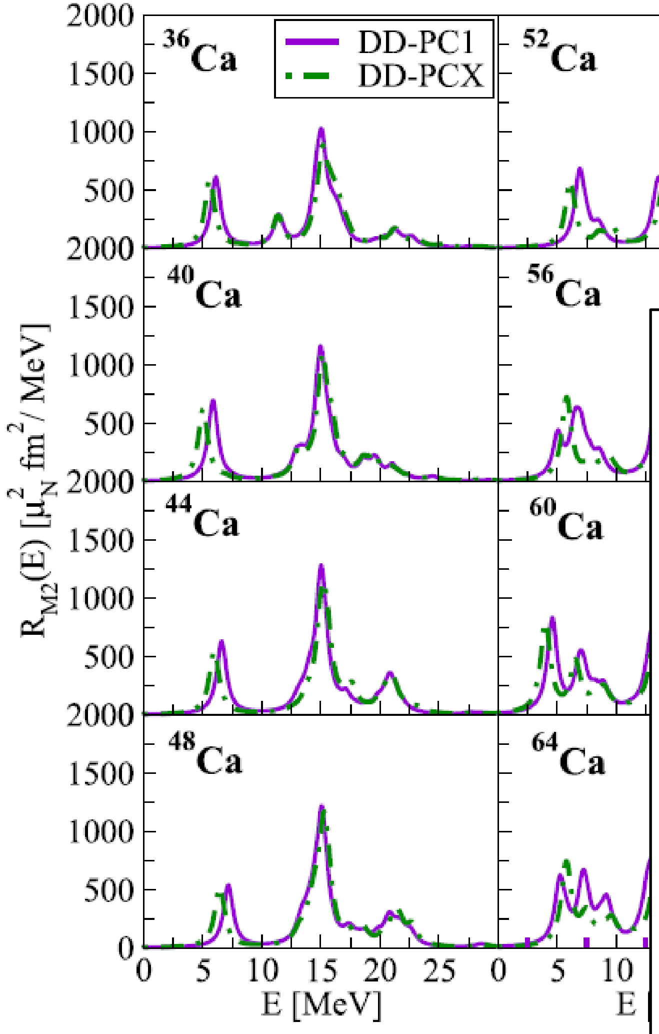

Fig. 7 The M2 full RQRPA response functions for C… for the DD-PC1 and DD-PCX interactions

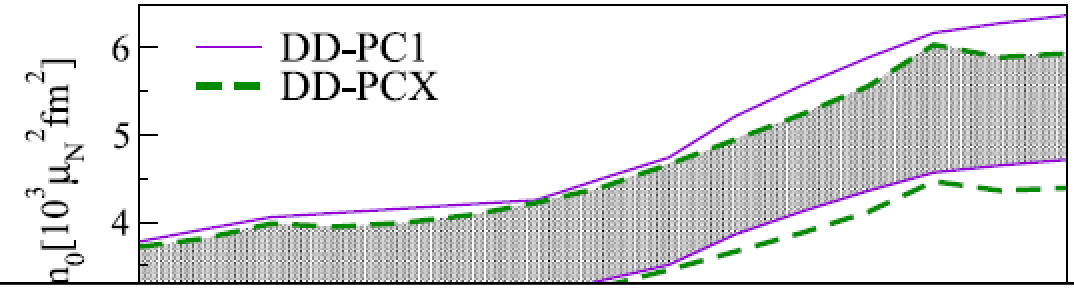

Conclusions in the M2 part: the relativistic HB+QRPA calculation is applied to the M1/M2 excitations.

✓ The IV-PV coupling as the residual interaction gives finite effects: ΔE = 2~5 MeV.

✓ Is the quenching effect common between M1 and M2? → for M2 especially, future experiments may provide the missing data to answer to this question.

Contents

Introduction for M1 transitions

Methods = REDF-QRPA

Topics

- M1 with QRPA
- Pairing sensitivity
- Gamow-Teller and M1
- M2 with QRPA

Summary of talk today

Summary and remaining problems for future studies

- ✓ M1 and GT transitions are calculated within the unique theoretical framework. → The simultaneous reproduction of M1/GT is still demanding. Why?

- ✓ M1 excitation of open-shell system is sensitive to the nuclear Cooper-pairing spin S_{12}. → What kind of pairing model is the best for open-shell nuclei?

- ✓ Calculations for M2 → When the M2 data will become available, can we use common quenching factor?

Announcement

Registration will be open soon.

原子核におけるスピン自由度の織り成すダイナミクス

11–13 Dec 2023
RCNP
Asia/Tokyo timezone

Enter your search term

- Overview
- Timetable
- Registration
- Participant List

[開催趣旨]

原子核はフェルミオンの多体系であり、スピン自由度が本質的な役割を果たす現象が数多く存在する。最も代表的なものは磁気多重極子およびGamow-Teller型の励起・遷移であり、核子のスピン反転を含む。スピン反転型の遷移は、元素合成プロセスや、二重ベータ崩壊などの原子核とニュートリノの反応を探る上でも、重要な手がかりを与える。しかし、その実態は完全には理解されていない。実験的には不安定核のGamow-Teller型励起や、二重Gamow-Teller共鳴、スピン双極子のクエンチングなどの解明が企図されている。理論的にも、残留相互作用、対相関、クエンチング効果、和則、１粒子１空孔を超えた励起成分の取り扱いなど、多くの問題が潜んでいる。有限核の磁気モーメントや密度分布とも密接に関連している。本研究会では、実験と理論のエキスパートが参集し、スピン自由度が関連する観測可能量に関して、現在までに判明した情報の整理・共有と、将来のアプローチについて議論する機会を提供する。

[世話人]

大石知広（世話人代表　理研仁科センター）
金田佳子（京大理）
民井淳 (阪大RCNP)
矢向謙太郎（東大CNS）
吉田賢市（阪大RCNP）